



University of Colorado
Boulder



Exploiting a high-rate trigger strategy at LHC: test of lepton flavor universality in $B \rightarrow \ell\ell K$

Georgios Karathanasis, on behalf of the CMS Collaboration

12/01/2023

- Introduction
 - Theoretical aspects
 - R_K definition and previous results
 - LHC and the CMS detector
- B Parking triggering strategy
 - Motivation
 - Implementation
 - Purity on B candidates
 - B Parking usage
- Main analysis
 - B candidate reconstruction
 - Selection of $B \rightarrow \mu\mu K$ candidates
 - Low p_T electron reconstruction
 - Selection of $B \rightarrow eeK$ candidates
 - $B \rightarrow \mu\mu X$ mass fits
 - $B \rightarrow eeX$ mass fits
 - Simultaneous mass fit $B \rightarrow \mu\mu K$ in q^2 bins
 - Systematic unc. and corrections
- Results
 - $d\text{BF}(B \rightarrow \mu\mu K)/dq^2$ measurement
 - $\text{BF}(B \rightarrow \mu\mu K)$ and R_K in $1.1 < m(\mu\mu)^2 < 6 \text{ GeV}^2$ measurements

Test of lepton flavor universality in $B^\pm \rightarrow K^\pm \ell^+ \ell^-$ decays

The CMS Collaboration

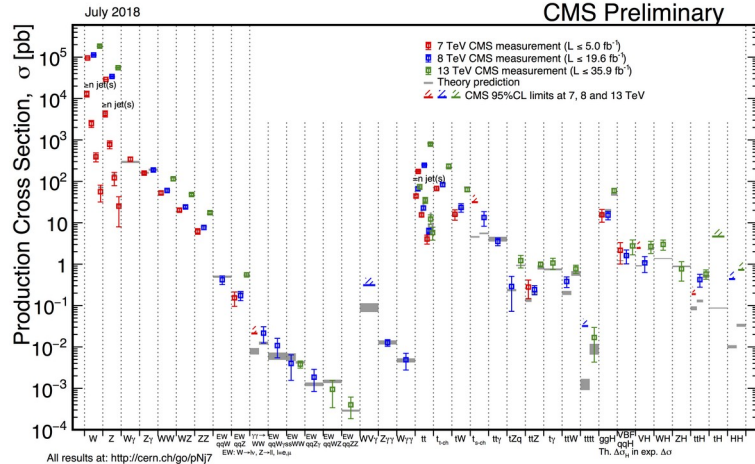
Abstract

A test of lepton flavor universality in $B^\pm \rightarrow K^\pm \ell^+ \ell^-$ decays, where ℓ is a muon or an electron, as well as a measurement of differential and integrated branching fractions of a nonresonant $B^\pm \rightarrow K^\pm \mu^+ \mu^-$ decay with the CMS experiment at the LHC are presented. The analysis is made possible by a dedicated data set of proton-proton collisions at $\sqrt{s} = 13 \text{ TeV}$ recorded in 2018, using a special high-rate data stream designed for collecting about 10 billion unbiased b hadron decays. The ratio of the branching fractions $\mathcal{B}(B^\pm \rightarrow K^\pm \mu^+ \mu^-)$ to $\mathcal{B}(B^\pm \rightarrow K^\pm e^+ e^-)$ is measured as a double ratio $R(K)$ of these decays to the respective branching fractions of the $B^\pm \rightarrow J/\psi K^\pm$ with $J/\psi \rightarrow \mu^+ \mu^-$ and $e^+ e^-$ decays, which allow for significant cancellation of systematic uncertainties. The ratio $R(K)$ is measured in a range $1.1 < q^2 < 6.0 \text{ GeV}^2$, where q is the invariant mass of the lepton pair, and is found to be $R(K) = 0.78^{+0.47}_{-0.23}$, in agreement with the standard model expectation within one standard deviation. This measurement is limited by the statistical precision of the electron channel. The integrated branching fraction in the same q^2 range of $\mathcal{B}(B^\pm \rightarrow K^\pm \mu^+ \mu^-) = (12.42 \pm 0.68) \times 10^{-8}$ is consistent with the present world-average value and has a comparable precision.

All plots and figures can be found here:

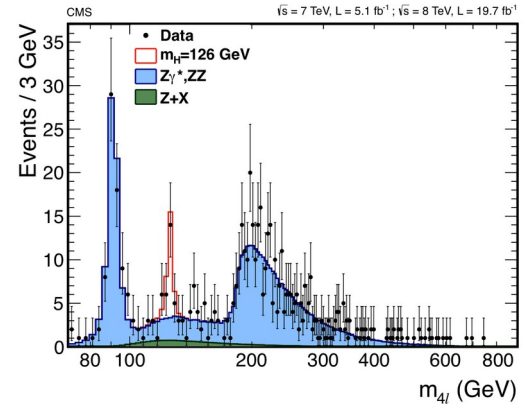
[BPH 22-005](#)

Introduction



Standard Model (SM):

- Encapsulates everything we know about Nature
- Successfully predicts processes in $\sigma [10^{-3} - 10^{11}] \text{ pb}$
- Discovery of Higgs Boson in 2012 led to extensive search of its properties \rightarrow (So far) no deviations from SM
- Yet, regarded as an “effective theory”



Not predicted/answered by SM

Hierarchy problem

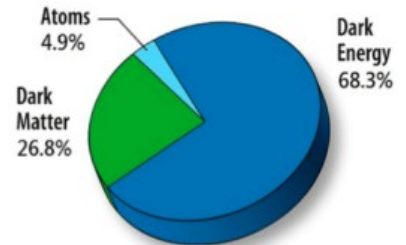
- New Physics at $\sim \text{TeV}$ scale or extremely fine-tuned Higgs mass?

Dark matter problem

- Astrophysical observations indicate 5 times larger mass than visible

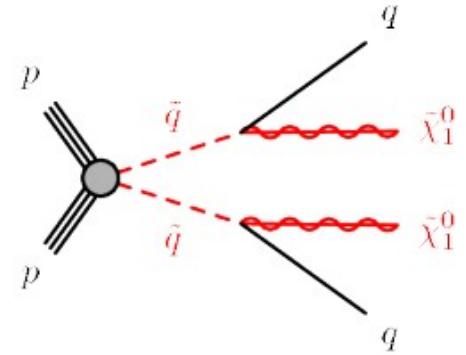
Many more that what can include:

- Neutrino oscillations
- Matter/antimatter asymmetry
- ...



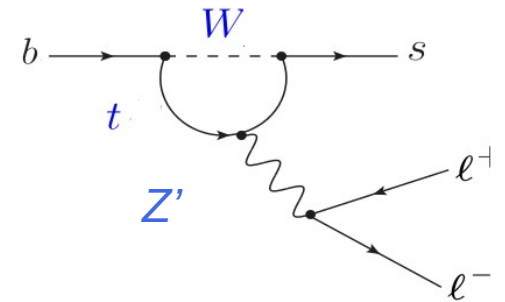
Direct searches:

- New particles are directly produced
- Targets specific Beyond SM (BSM) theory
- (Usually) on-mass shell particles \rightarrow large signal expected
- Bounded by the center of mass of LHC collisions
- Variety of signatures

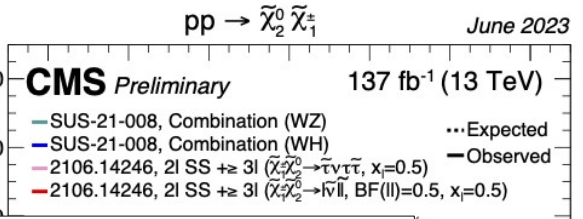
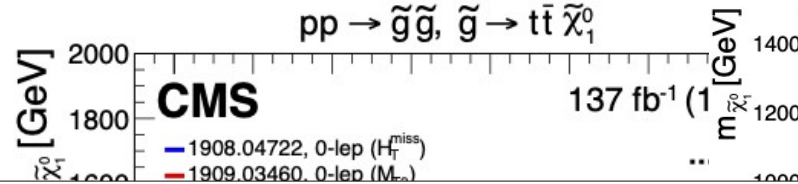
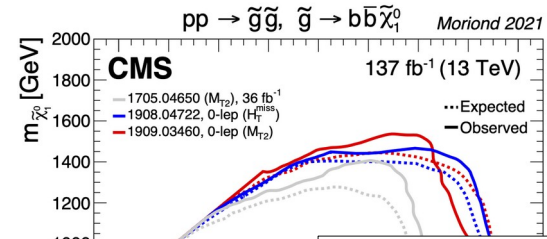


Indirect searches:

- New particles are produced only in loops
- Effects can be explained by many BSM models
- Not bounded by the center of mass of LHC
- Small number of events expected
- Focusing on rare SM signatures where small BSM contributions can be visible.

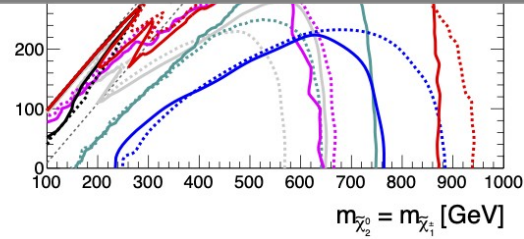
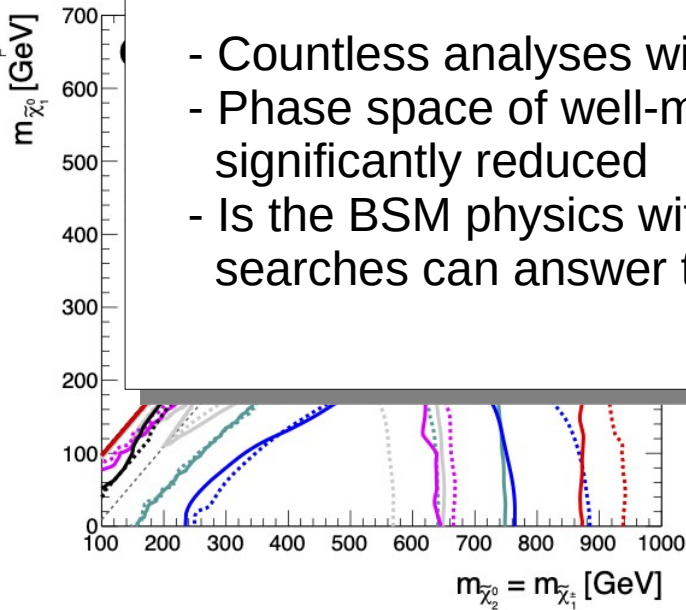


Status of Beyond SM direct searches



Status of direct searches:

- Countless analyses with no evidence of BSM so far
- Phase space of well-motivated theories, like SUSY significantly reduced
- Is the BSM physics within LHC reach? \rightarrow focus on indirect searches can answer this

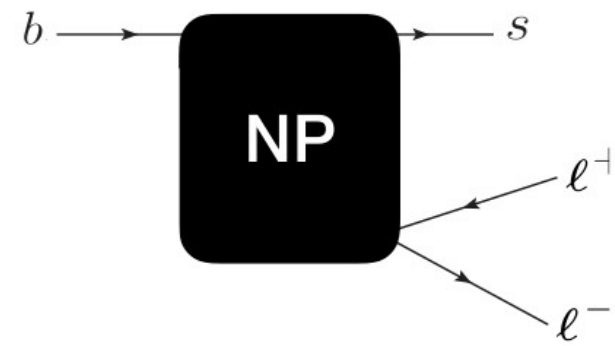
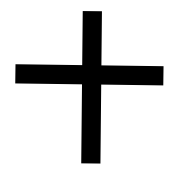
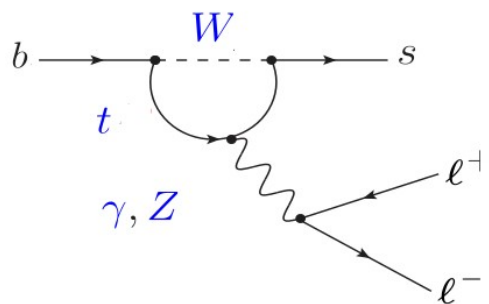
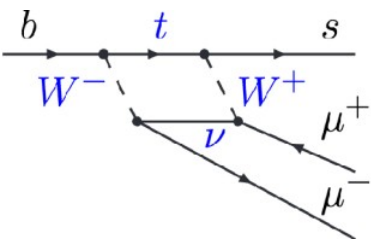


Interest in $b \rightarrow sll$ transitions

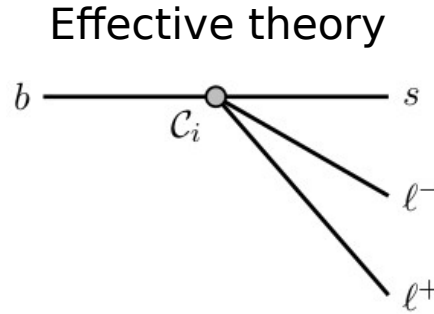
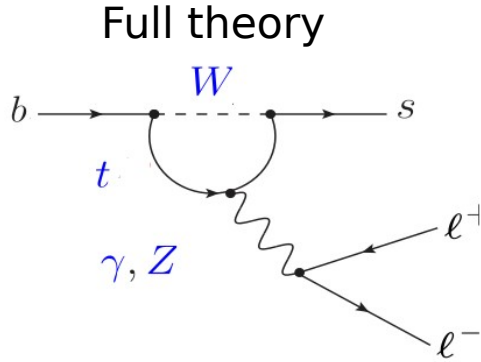
- So far no BSM physics has been observed from direct searches
- Rare decays: powerful tool for indirect searches

- $b \rightarrow sll$ transition in the SM:
 - Prohibited at tree level (FCNC)
 - Via loop diagrams (eg penguin, box)
 - Very rare \rightarrow Weak signals in BSM might be visible

- Quantities affected by the BSM:
 - Lepton flavour universality (LFU)
 - Branching ratios (BR)
 - Differential BR
 - Angular distributions



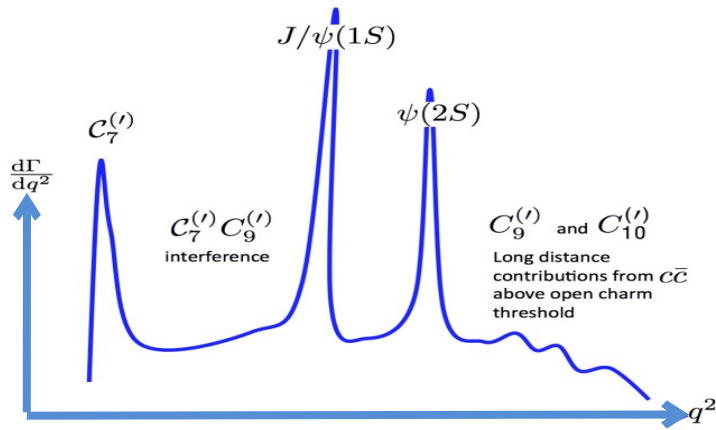
Describing $b \rightarrow s l l$ with Effective Theory



$b \rightarrow s l l$ described in model independent effective theory

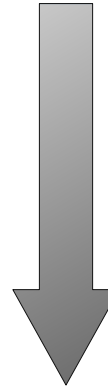
$$\mathcal{H}_{\text{eff}} = \frac{-4 G_F}{\sqrt{2}} V_{tb} V_{ts}^* \frac{e^2}{16 \pi^2} \sum_i C_i O_i$$

↓
Wilson coefficients



Different $q^2 = m(l, l)^2 \rightarrow$ different C_i probed

Prediction accuracy



Limitations on SM predictions:

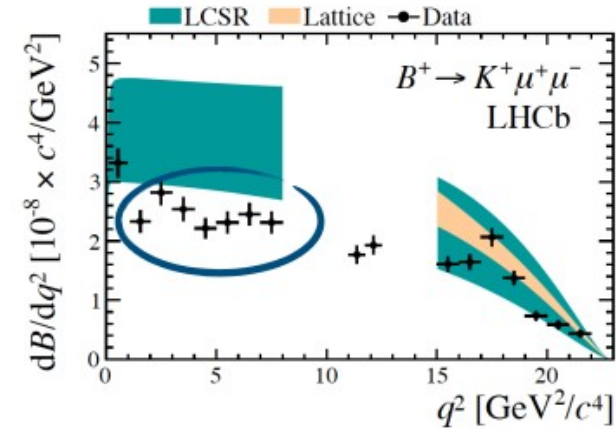
- BF measurements affected by:
 - form factors and c-c loops
- Angular distributions affected by:
 - only c-c loops
- LFU ratios affected by:
 - neither form factors nor c-c loops

LFU test with minimal theoretical uncertainty via the $B \rightarrow \mu\mu K$ to $B \rightarrow eeK$ ratio, R_K :

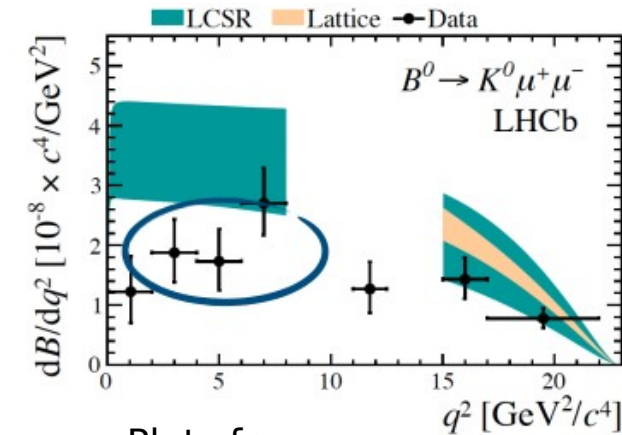
$$R_K = \frac{BF(B \rightarrow \mu\mu K)}{BF(B \rightarrow eeK)}$$

To reduce experimental uncertainties \rightarrow divide both numerator and denominator with $BF(B \rightarrow J/\psi K)$. R_K becomes:

$$R_K = \frac{BF(B \rightarrow \mu\mu K)}{BF(B \rightarrow J/\psi K, J/\psi \rightarrow \mu\mu)} / \frac{BF(B \rightarrow eeK)}{BF(B \rightarrow J/\psi K, J/\psi \rightarrow ee)}$$

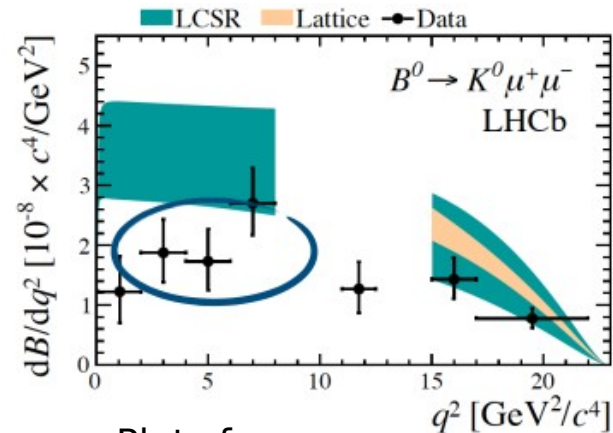
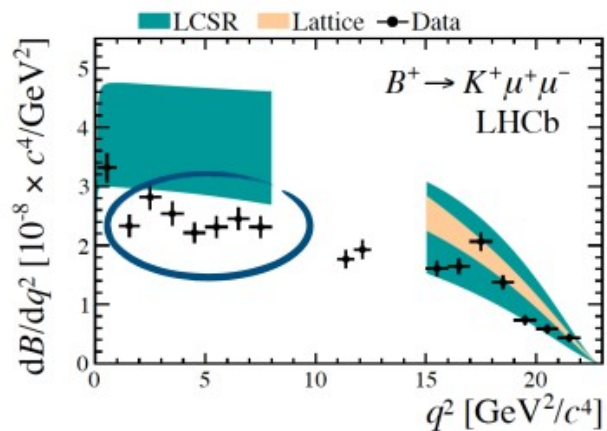


- Deviations of measurements and SM expectations in dB/dq^2 :
 - Seen in several channels
 - Hadronic form factors have large uncertainties
 - BSM effect or common issue of SM expectation?



- Furthermore several angular measurements show $\sim 3\sigma$ deviations from SM expectation
- Intriguing pattern

Plots from [JHEP 1406 133](#)



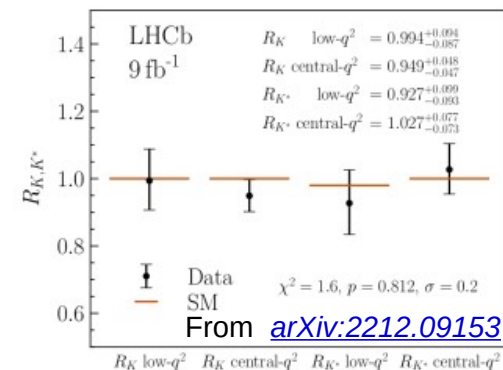
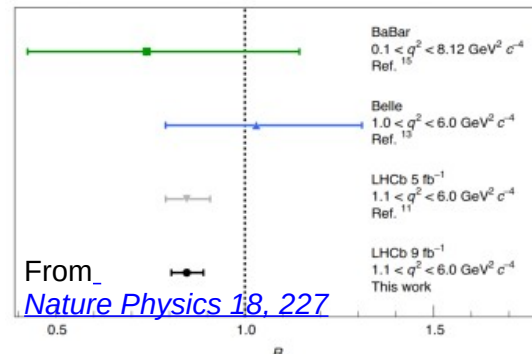
Plots from [JHEP 1406 133](#)

- Deviations of measurements and SM expectations in dBF/dq^2 :
 - Seen in several channels
 - Hadronic form factors have large uncertainties
 - BSM effect or common issue of SM expectation?

- Furthermore several angular measurements show $\sim 3\sigma$ deviations from SM expectation

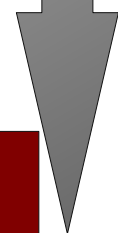
- Intriguing pattern

Where we “stand” in R_K ?



Today: the 1st R_K result from CMS using Run 2 data

time

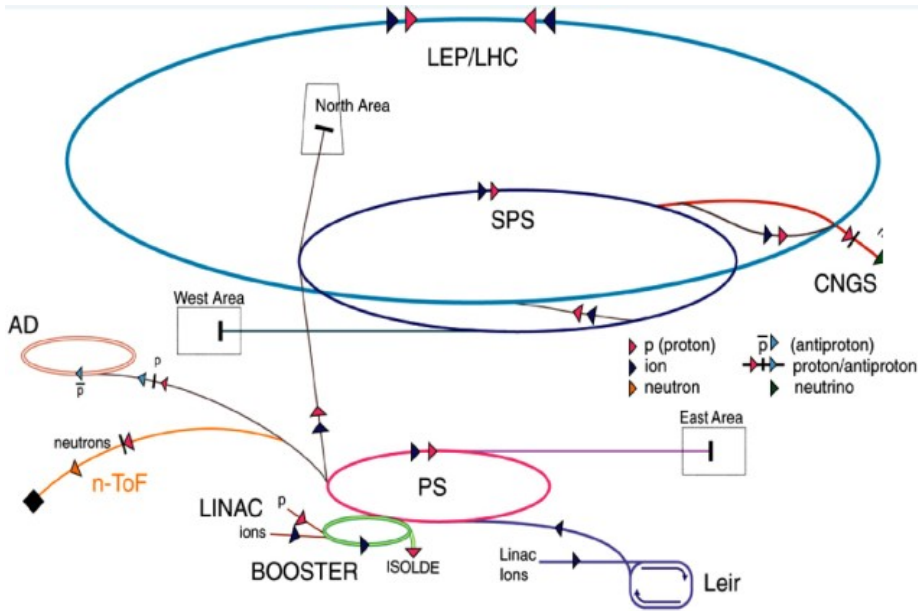


The Large Hadron Collider



Large Hadron Collider

- Most powerful accelerator
- 27-kilometer ring
- Located in Switzerland & France
- 2 proton beams colliding at 13 TeV
- 4 Interaction points:
ATLAS, CMS, LHCb, Alice

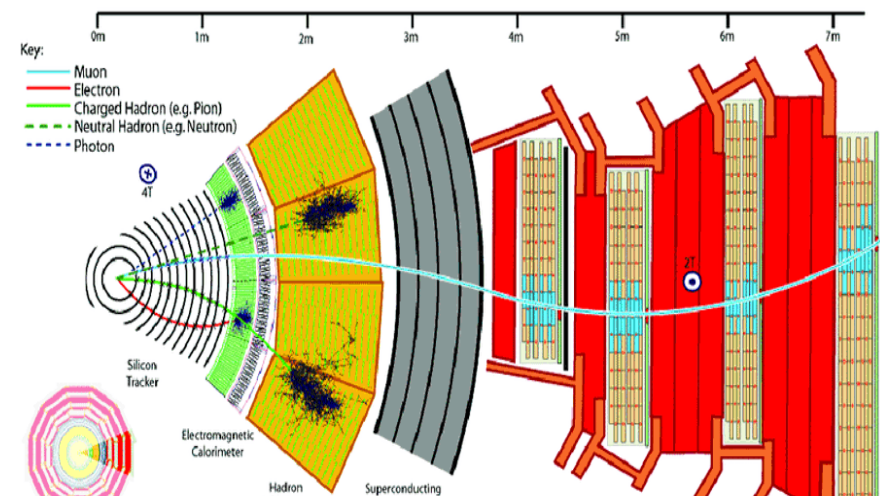
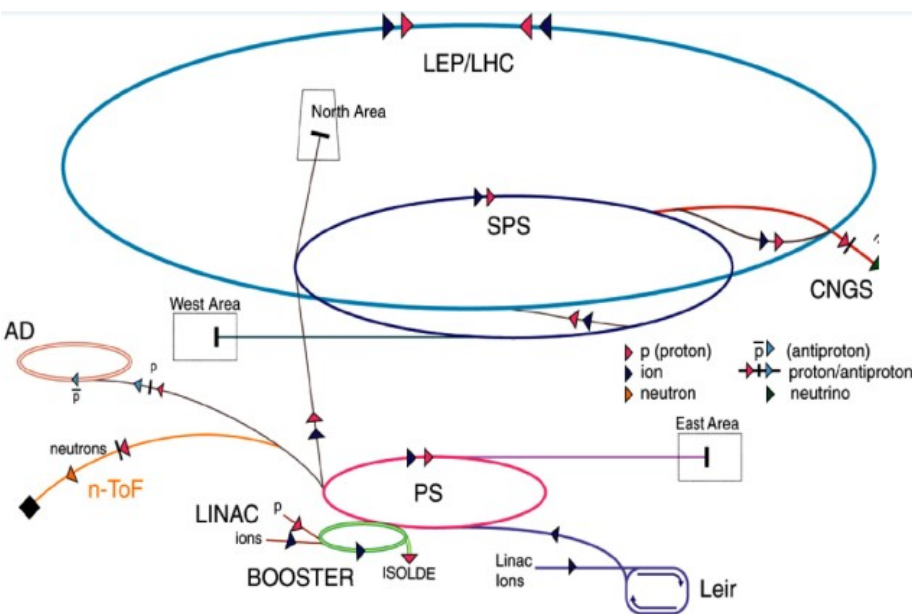


The Compact Muon Solenoid



Large Hadron Collider

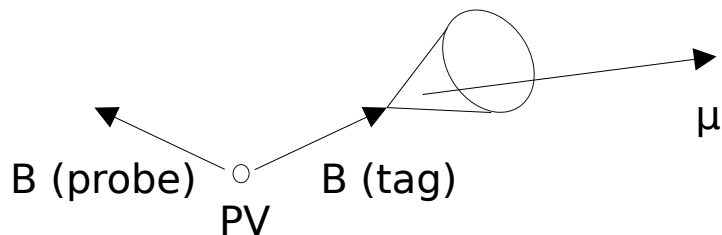
- Most powerful accelerator
- 27-kilometer ring
- Located in Switzerland & France
- 2 proton beams colliding at 13 TeV
- 4 Interaction points:
ATLAS, **CMS**, LHCb, Alice



Compact Muon Solenoid

- Located near Cessy
 - Magnet generates 3.8 T
 - General purpose experiment
 - Detectors (from inside out):
Tracker, electromagnetic calorimeter,
hadronic calorimeter, muon chambers
- More information in the [TDR](#)

B – Parking strategy



Event collection:

- **Use one b-hadron to trigger, while the other decays freely**
- $BF(b \rightarrow \mu X) \sim 20\%$: large fraction in a very clean object
- Use μ -based paths to trigger
- This technique is known as Tag-and-Probe
- Tag = triggering B

Back-of-the-envelope estimation:

$$N = f_B * BF(B \rightarrow eeK) * R_{HLT} * P_{HLT} * T$$

Where:

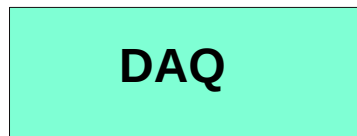
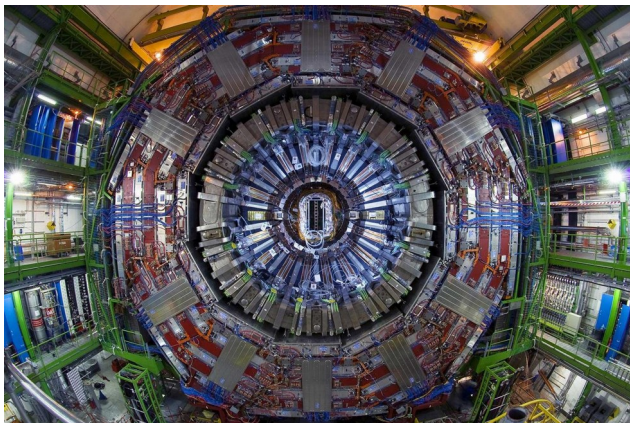
- N = Produced events
- $BF(B \rightarrow eeK) \sim O(10^{-7})$
- f_B = B hadron type fraction (0.4)
- R_{HLT} = Trigger rate (~ 2 kHz)
- P_{HLT} = Trigger purity ($\sim 75\%$)
- T = HLT active time

Aim for **$N \sim 300$ events**

$$\Rightarrow T = 1.11 \times 10^6 \text{ sec}$$

To collect 300 eeK events $\sim 10 \times 10^9$ B events needed

Collisions (p - p) at 40 MHz



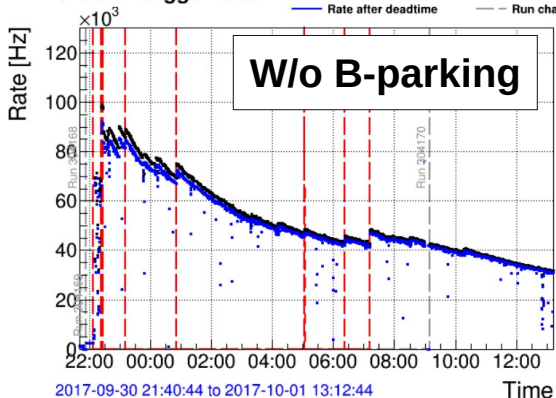
- Single- μ L1 seeds
- η restricted, soft p_T
- Purity in B decays $\sim 30\%$
- Constant L1 rate

- L1 seeds as inputs
- Refined p_T and d_{xy} cut

- Saved in single copy
- Stored on tape until computing resources available
- Long delay in reconstruction; procedure known as "Parking"

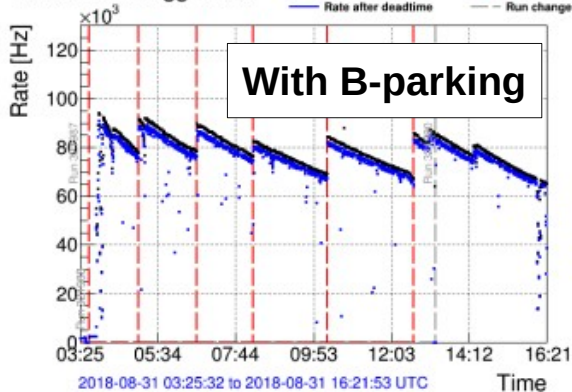
Fill 6259 L1 trigger rate

— Rate before deadtime
— Rate after deadtime
- - Prescale change
- - Run change



Fill 7108 L1 trigger rate

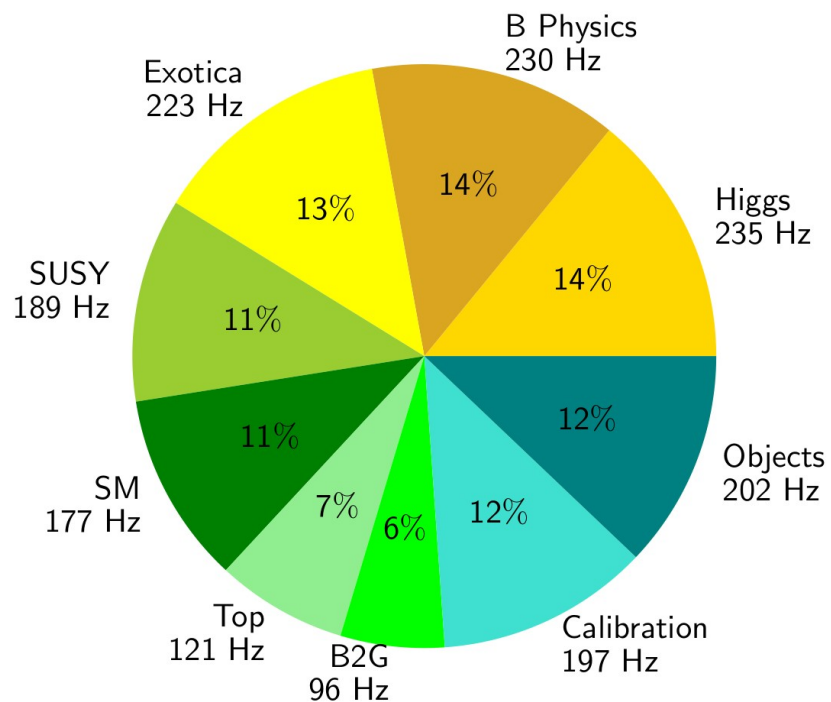
— Rate before deadtime
— Rate after deadtime
- - Prescale change
- - Run change



- As luminosity decreases lower p_T seeds enabled
- Tune/optimize paths during data-taking
- **Collected during 2018**

“standard CMS menu” HLT rate

CMS Preliminary (13 TeV, 2018, $2.0 \times 10^{34} \text{ cm}^{-2} \text{ s}^{-1}$)



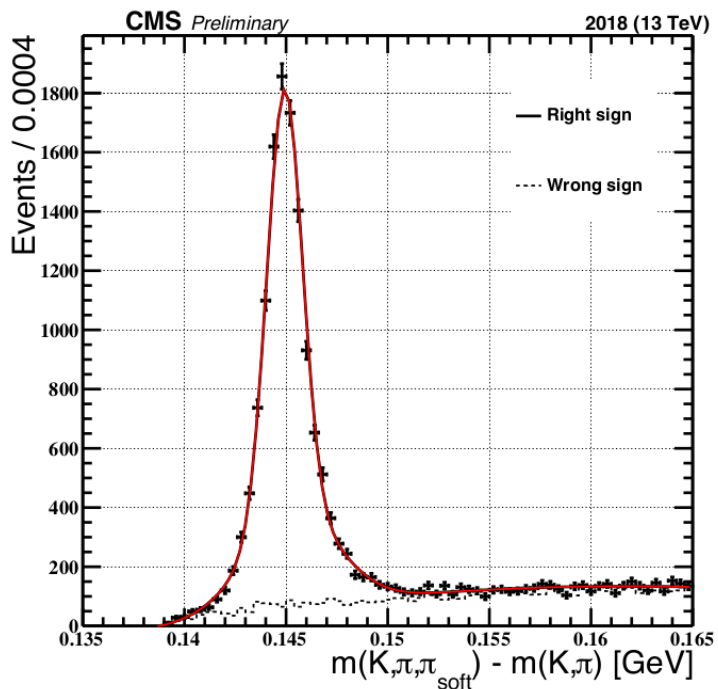
- In 2018 all B Physics rate was coming from muon-based triggers
- With 230 Hz, the number of probe $B \rightarrow eeK$ produced is <30
- Adding acceptance & reconstruction factors, negligible number of events expected
- Using a parking strategy was the only way to measure R_K

Purity in B candidates



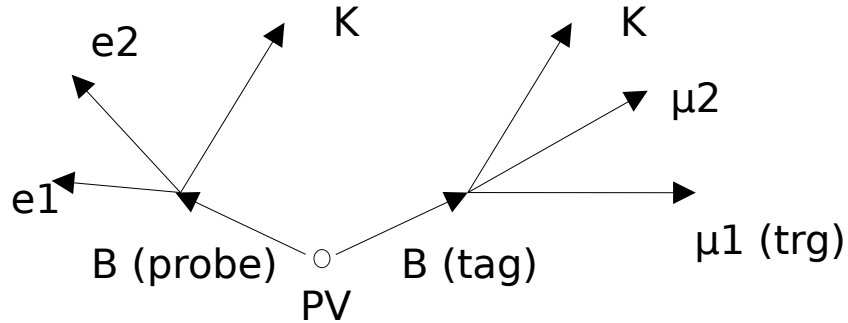
- D^0 built by combining tracks of opposite charges, that pass some selection
- D^* built by combining D^0 candidates with a soft track
- Measure P_b for the HLT_Mu9_IP6: μ is required to pass this trigger
- Right Sign, RS: $Q(\mu) \neq Q(\pi_s)$ [Signal] ; Wrong Sign, WS: $Q(\mu) = Q(\pi_s)$ [BKG]
- Plotting $M(K, \pi, \pi_s) - M(K, \pi)$ creates a distinctive peak

More information in
[DP 19-043](#)

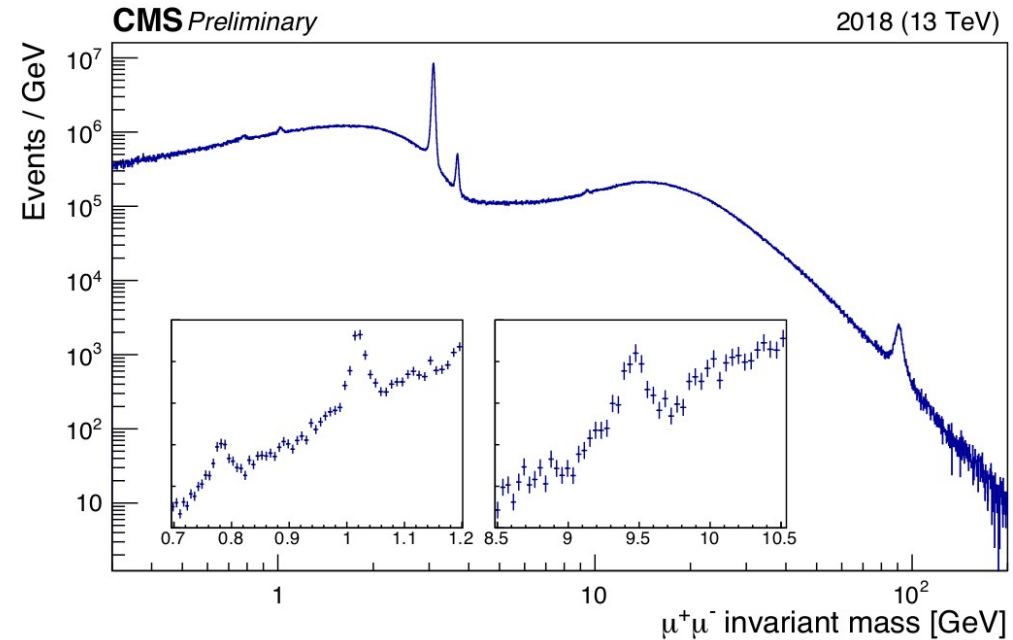


$$P_b = \frac{(N(b \rightarrow \mu))}{(N(\mu))} = \dots \implies P_b = 0.73$$

- In R_K analysis both $B \rightarrow \mu\mu K$ and $B \rightarrow eeK$ needed
- $B \rightarrow \mu\mu K$ comes from the “tag B” to improve statistics
- $B \rightarrow eeK$ from the “probe B”



- B Parking sample: powerful tool used by many analyses
- Single displaced muon trigger: used in Exotic and B physics with muon(s) in final state
- “probe B” used for non-triggered decays



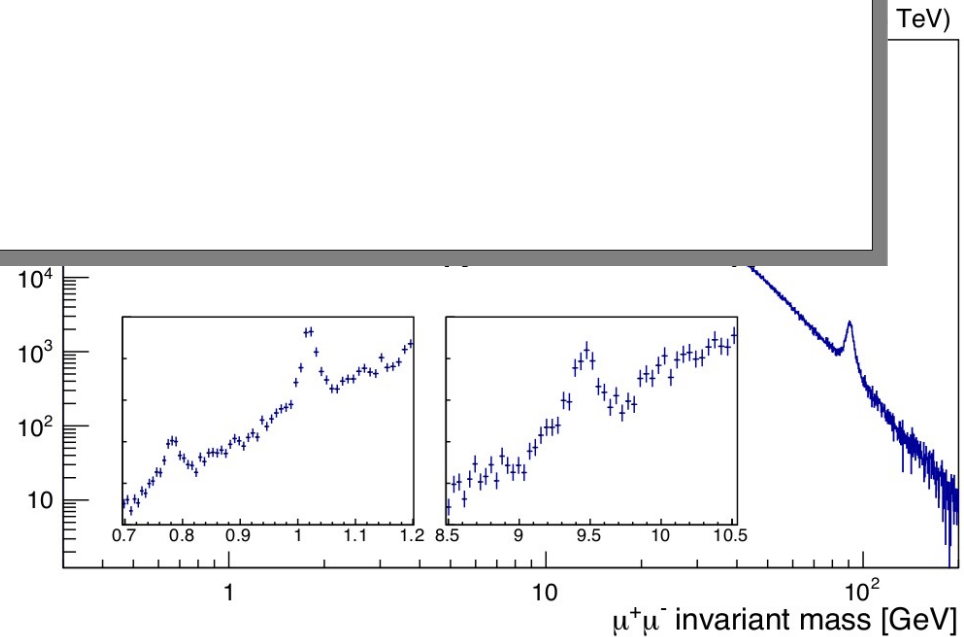
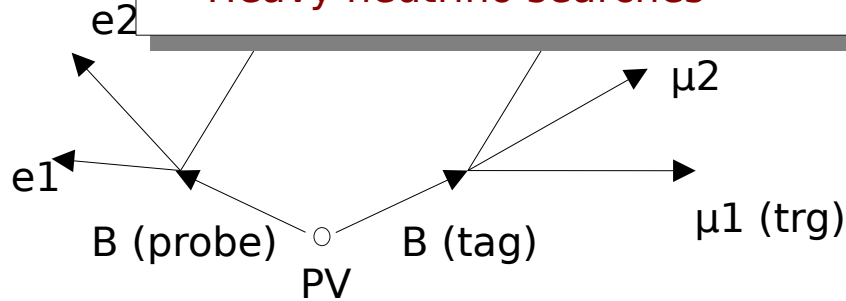
Usage of B Parking sample

- In R_K analysis both $B \rightarrow \mu\mu K$ and $B \rightarrow eeK$ needed
- $B \rightarrow \mu\mu K$ comes from the “tag B” to improve statistics
- $B \rightarrow e\mu K$

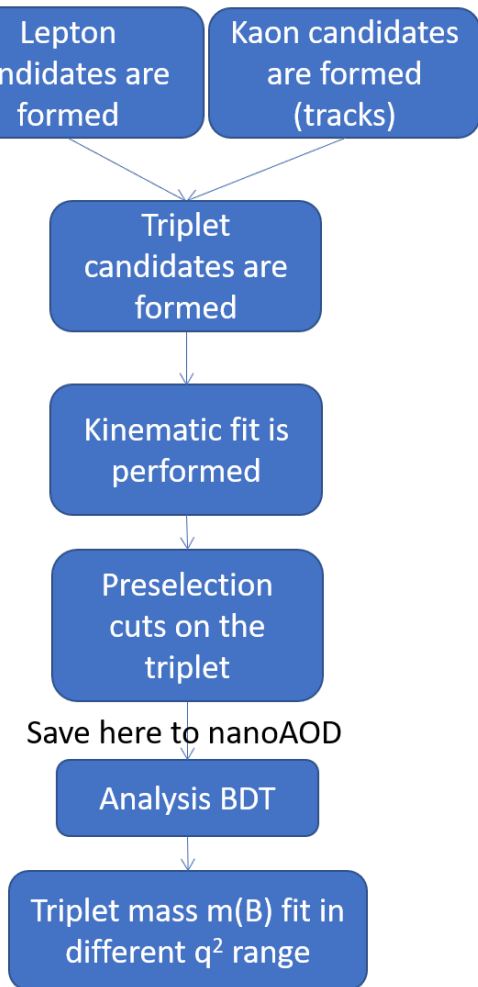
- B Parking sample: powerful tool used by many analyses
- Single displaced muon trigger: used in Exotic and B physics with muon(s) in final state

B Parking sample is used for more analysis than R_K :

- $R(D)/R(D^*)$ measurement
- CP violation studies
- Exotic searches
- Rare B decays
- Heavy neutrino searches



Main analysis



A practical problem: Running on 10^{10} events requires a lot of storage, time and computing power

Analysis framework strategies:

- 1) Apply preselection cuts as early as possible in the chain
- 2) Move time consuming processes at the end
- 3) Modify the precision of ntuple variables to reduce size

Preselection cuts:

- Optimized using using adaptive grid search (back up)

Selection:

- Based on Boosted Decision Trees (BDT) with [*XGBoost*](#)

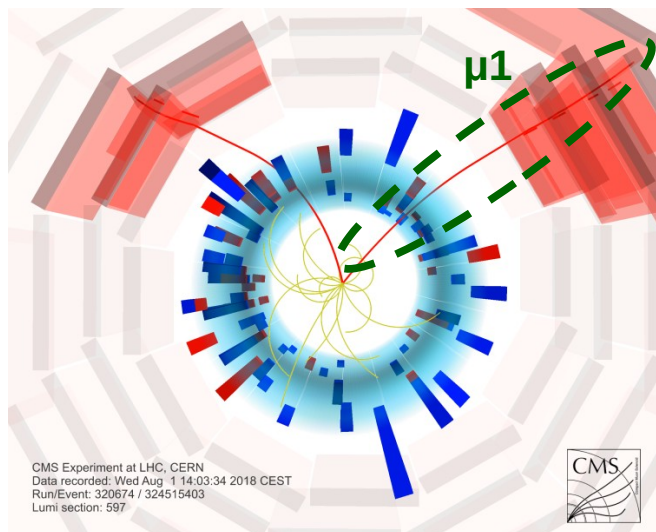
Fits:

- All mass fits are unbinned max likelihood fits, using [*RooFit*](#)

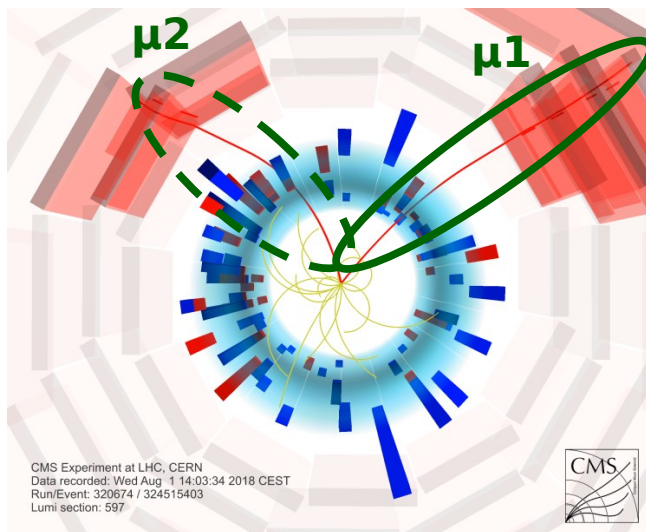
Reconstructing B candidates

All events are collected by the single μ parking triggers

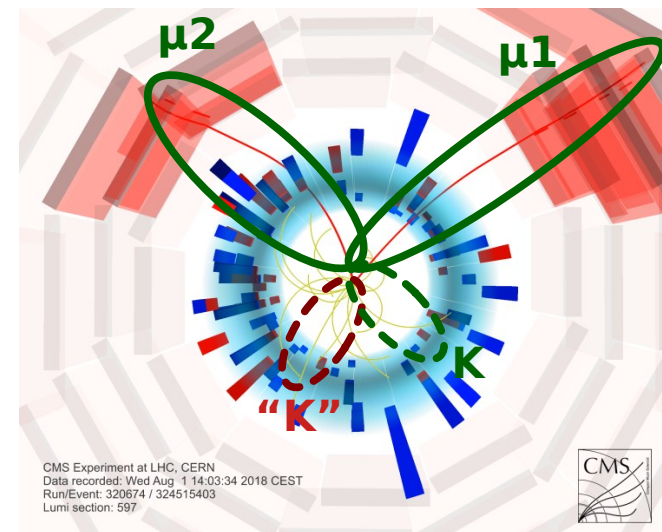
Step 1: Find the triggering muon



Step 2: Select μ close in z to triggering $\mu \rightarrow$ dilepton candidates with $m < 5\text{GeV}$



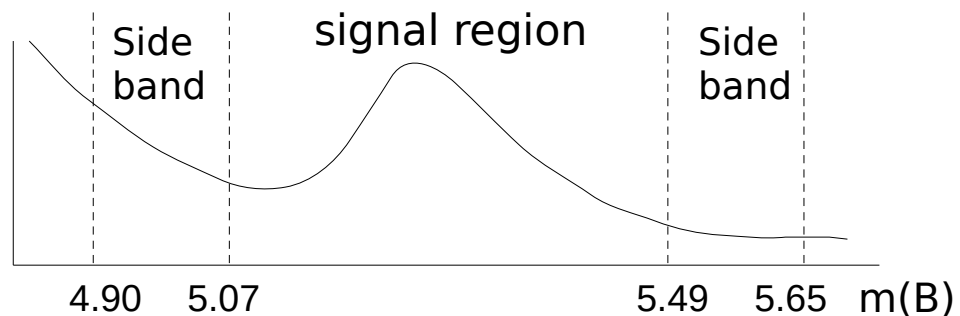
Step 3: Select tracks close to dilepton; assign $m(K)$ and kinematically fit to build B candidates



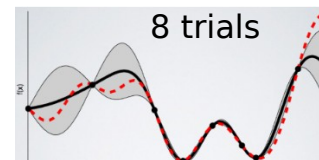
- Events can have more than 1 candidate

BDT optimization strategies

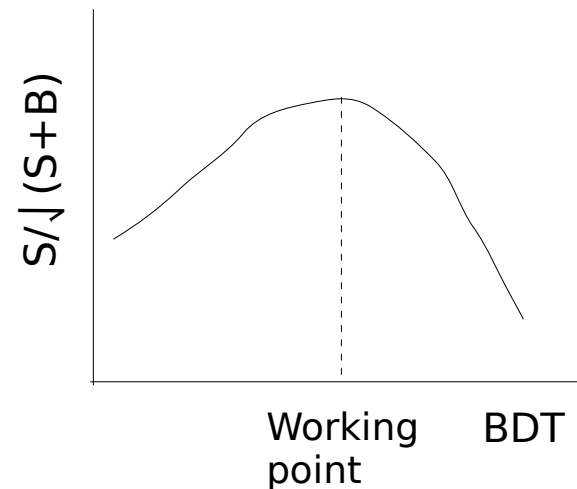
- Main selection based on BDT
 - 8-fold cross-validation structure
 - Data sidebands as background
 - Simulated (MC) $B \rightarrow \ell\ell K$ as signal



- Optimization
 - Input variables
 - Configuration options (hyperparameters)
 - Tested for “mass sculpting”
 - Working point defined as the value that Maximizes the $S/\sqrt{S+B}$ of the signal



Hyperparameters optimization



Same techniques/methods but different BDTs for μK and eeK states

Selection of $B \rightarrow \mu\mu K$ candidates

Object selection:

- Muons: Medium ID, $p_T(\mu_1) > 9$ GeV, $p_T(\mu_2) > 2$ GeV and $|\eta| < 2.4$
- Tracks: “High purity” ID, $p_T > 1$ GeV and $|\eta| < 2.4$

BDT variables

$\min \Delta R(\mu, K^+)$ $\cos \alpha_{3D}$

$\min \Delta z(\mu, K^+)$ $p(B^+ \text{ vtx})$
 L_{xy}/σ_{xy}

$\text{ISO}(\mu_{\text{lead}})$ $p_T(B^+)$

Only on $B \rightarrow \mu\mu K$
BDT

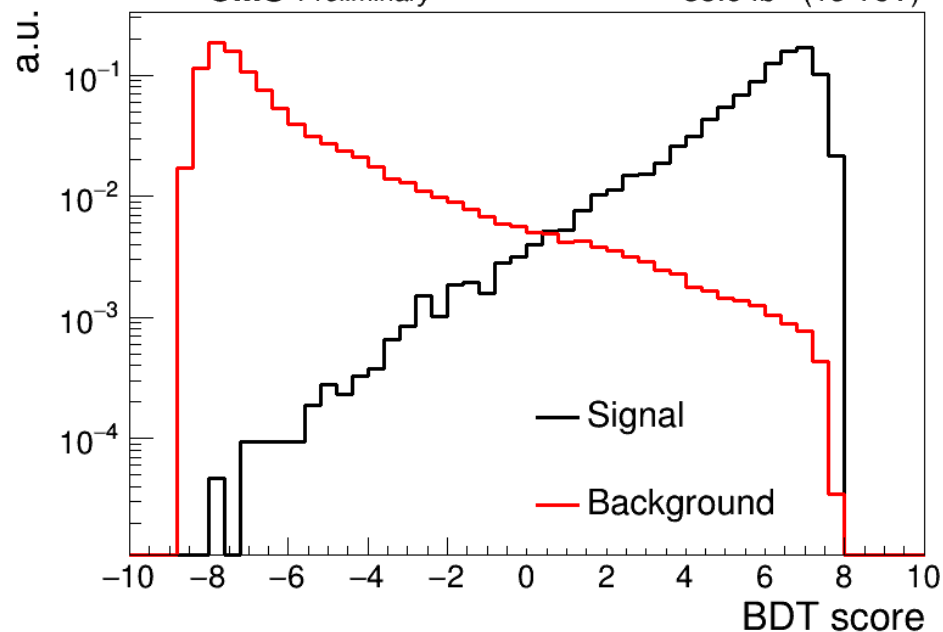
$p_T(K^+)$

Common in $B \rightarrow eeK$ and $B \rightarrow \mu\mu K$
BDTs

BDT discriminant for $B \rightarrow \mu\mu K$

CMS Preliminary

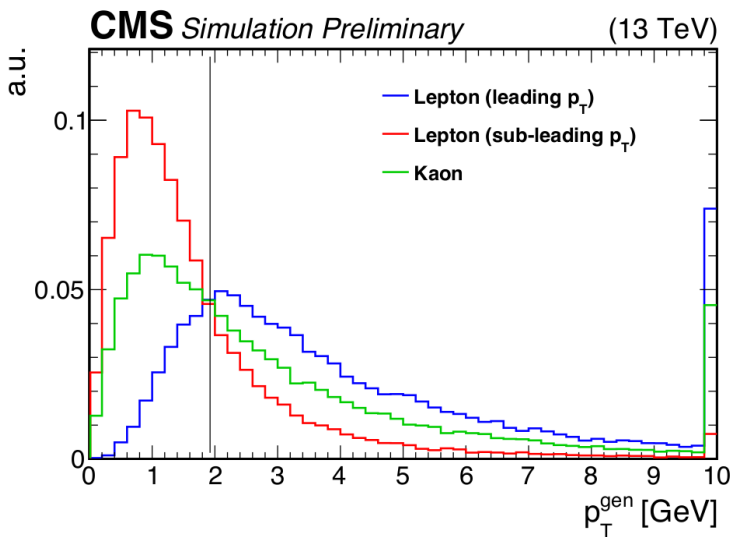
33.6 fb⁻¹ (13 TeV)



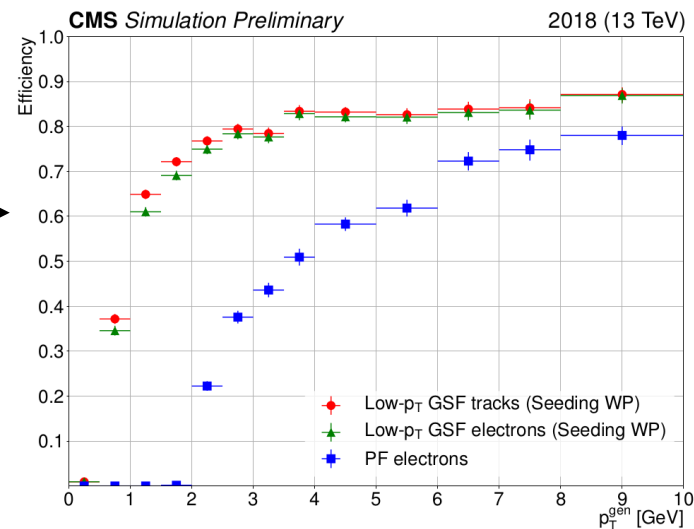
Motivation:

- Most B produce e with $p_T < 2\text{ GeV}$
- Cannot be reconstructed with the “standard” algo (particle flow, PF)

- More information in [DP 19-043](#)
- Low p_T e:
- Tracker seeded
 - e candidates identified MVA methods
 - Gain in efficiency for $p_T(e) < 5$
 - **Introducing more background** (including from B decays).



Created a new type of electron the “low p_T ” (LP)



Selection of $B \rightarrow eeK$ candidates

Object selection:

- Electrons: Candidates with two PF electrons (PF - PF) or one PF and one LP (PF - LP)
- Tracks: Same as in $B \rightarrow \mu\mu K$ case

2 BDTs trained:
one for PF - PF candidates
and one for PF - LP candidates

Variables exclusive to $B \rightarrow eeK$ BDT

$$p_T(e_{1,2})m_{K^+e^+e^-}$$

$$ID(e_{1,2})$$

$$\Delta z(e_{1,2}, K^+)$$

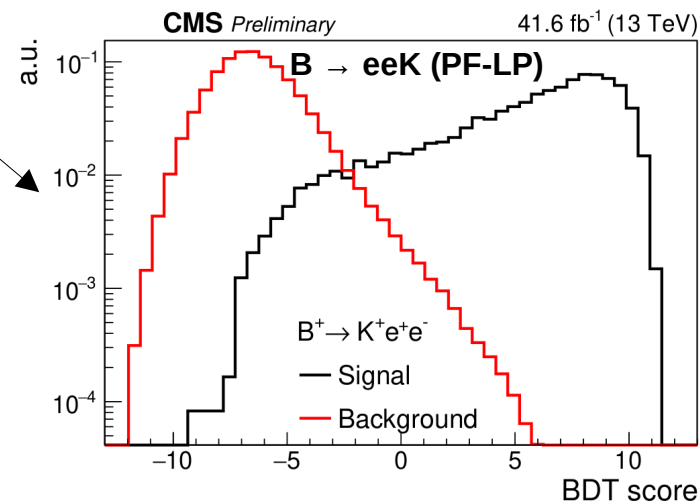
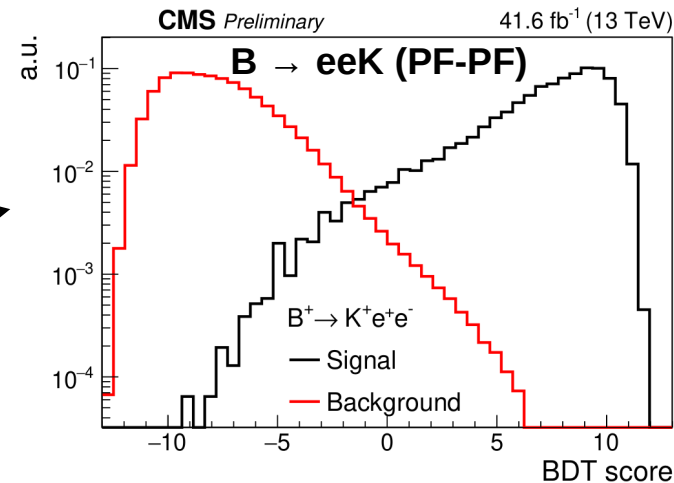
$$I_{\Delta R=0.4}^{\text{rel}}(e_1/e_2/K^+)$$

$$|d_{3D}(K^+, e^+e^-)| / \sigma_{|d_{3D}(K^+, e^+e^-)|}$$

$$\Delta R(e^+, e^-)$$

$$\Delta R(e_{1,2}, K^+)$$

$$\frac{|\mathbf{p}(e^+e^-) \times \mathbf{r}| - |\mathbf{p}(K^+) \times \mathbf{r}|}{|\mathbf{p}(e^+e^-) \times \mathbf{r}| + |\mathbf{p}(K^+) \times \mathbf{r}|}$$

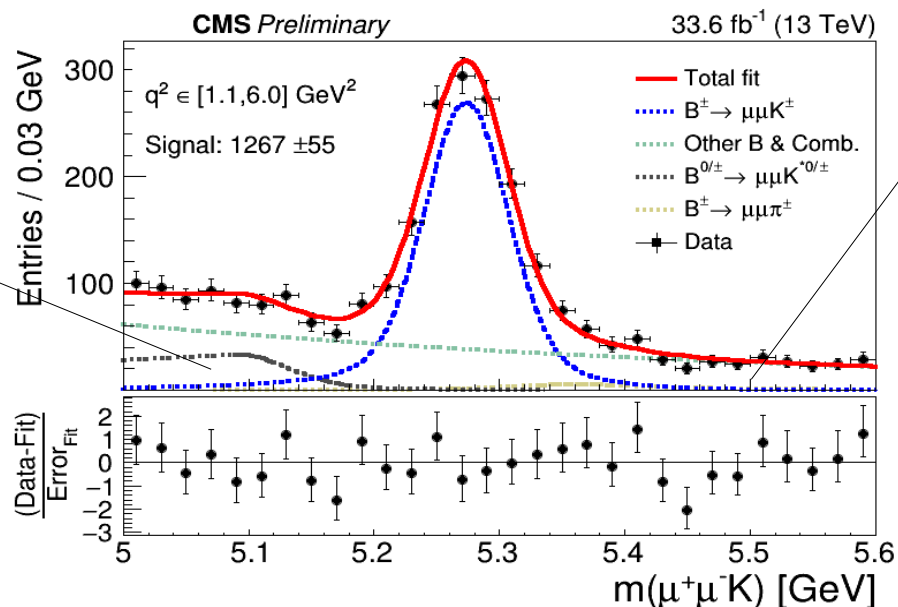


Background composition

The backgrounds are divided in two categories based on the type:

- Partial B: Candidates from partial reconstruction of B meson decays with many tracks
- Combinatorial: Candidates created with 1 or more objects from pile up/other B

Example using $B^\pm \rightarrow \mu\mu K^\pm$

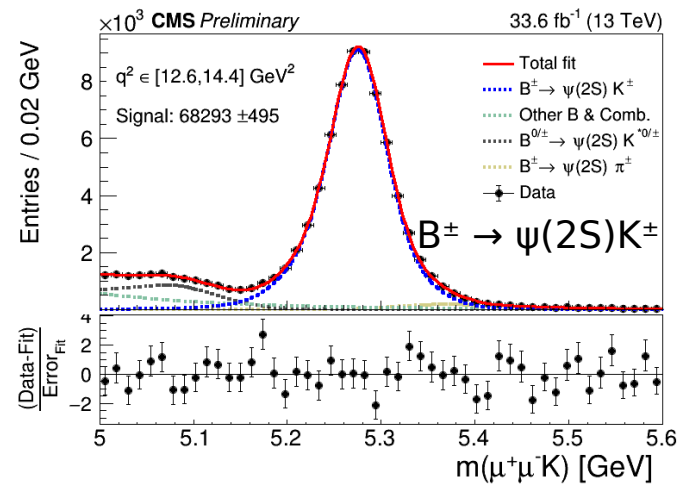
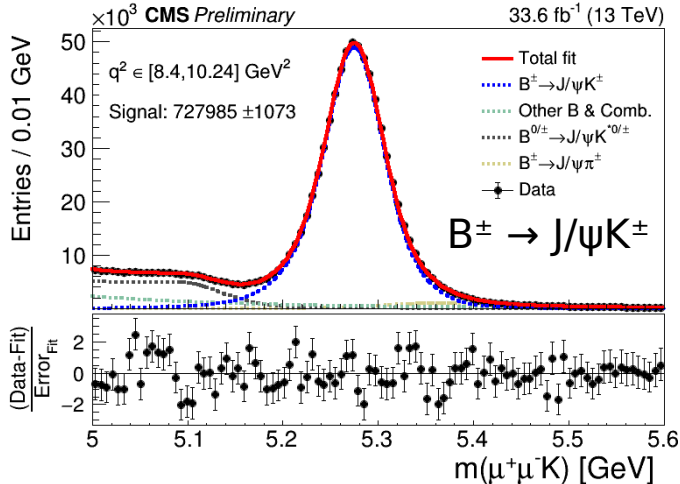
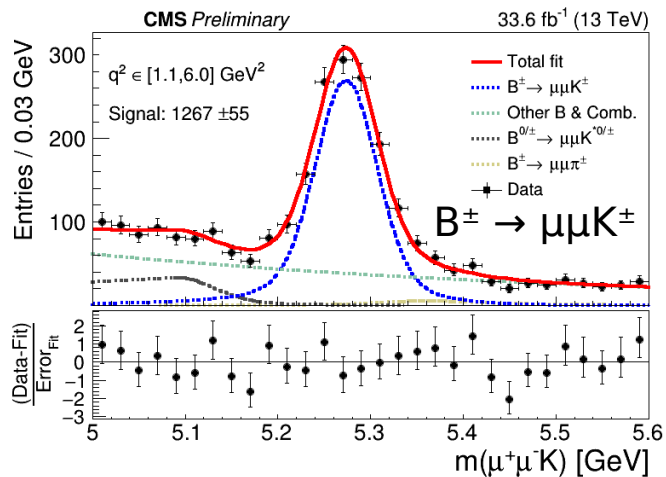


Partial B:
- Dominated by $B \rightarrow \mu\mu K^*$
- Lower mass than $m(B)$

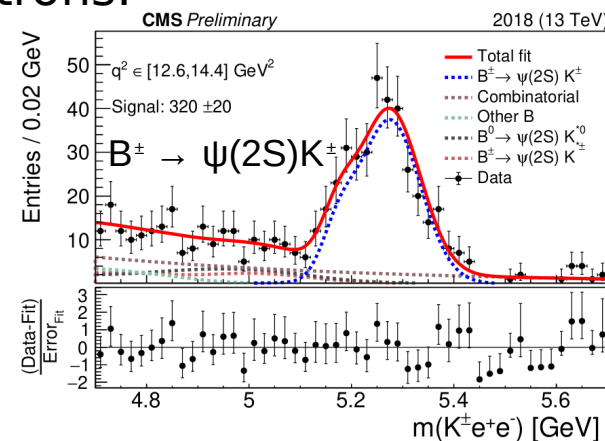
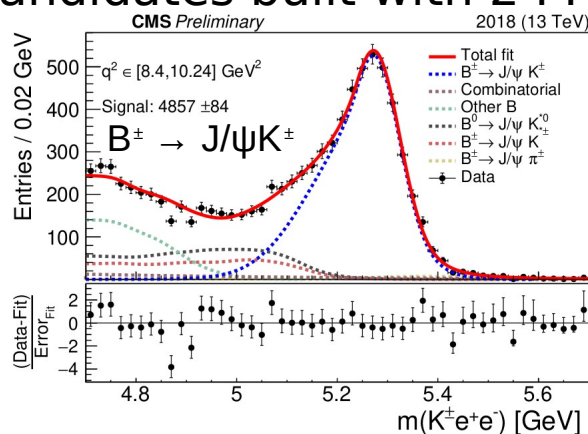
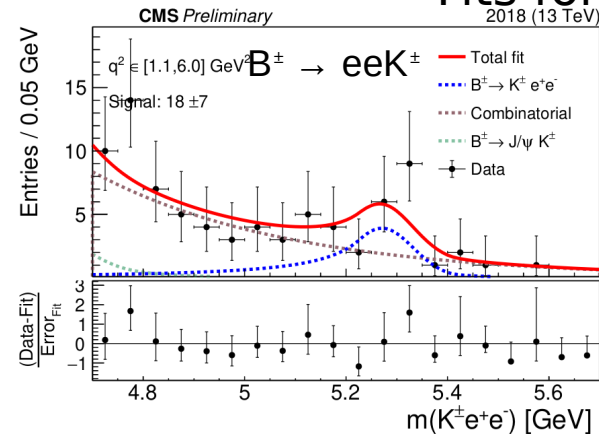
Combinatorial:
- Only background in signal region
- Dominates the high mass sideband
- Studied using B candidates with same sign leptons

B → μμX mass fits

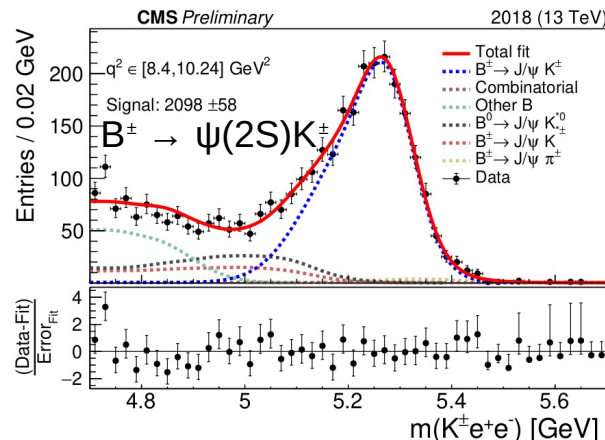
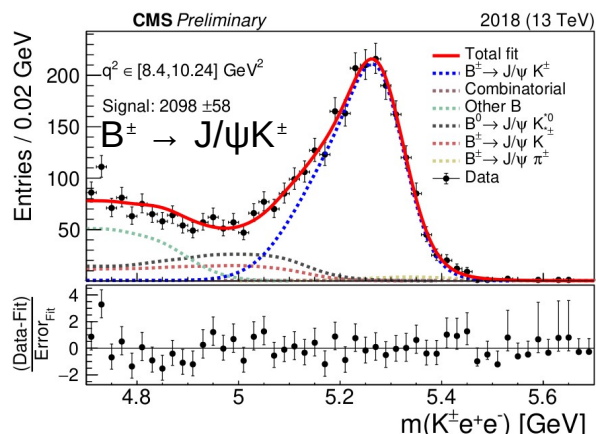
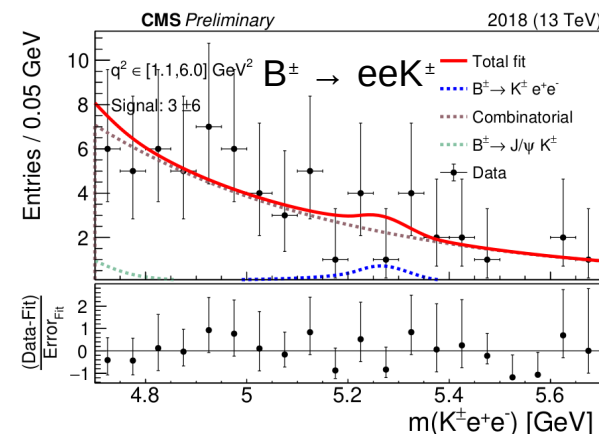
- Analytical functions used for fitting signal and backgrounds
- Signal:
 - Combination of Gaussians and Double-Sided Crystal Ball functions
- Backgrounds:
 - B → K*ll: partial reconstruction of the dominant 4 body decay
 - Other B: Any other B decay (sequential or J/ψX)
 - Combinatorial: random combinations of objects from B decays
 - J/ψK leakage (relevant only in eeK)



Fits for B candidates built with 2 PF electrons:



Fits for B candidates built with 1 PF & 1 LP electrons:



B \rightarrow $\mu\mu$ K mass fits in q^2 bins

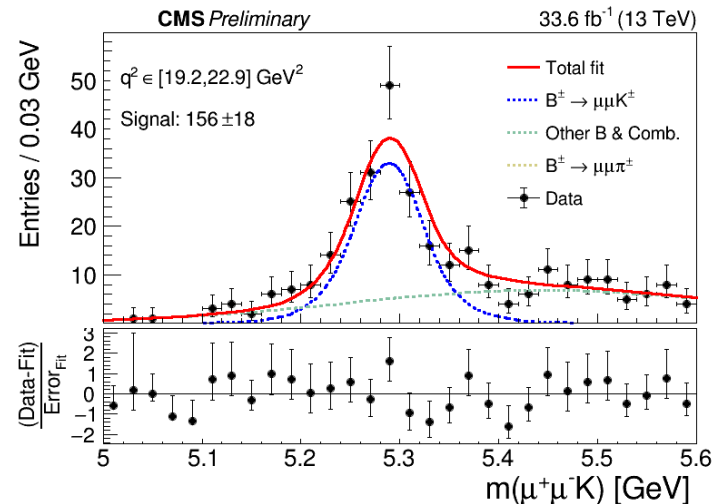
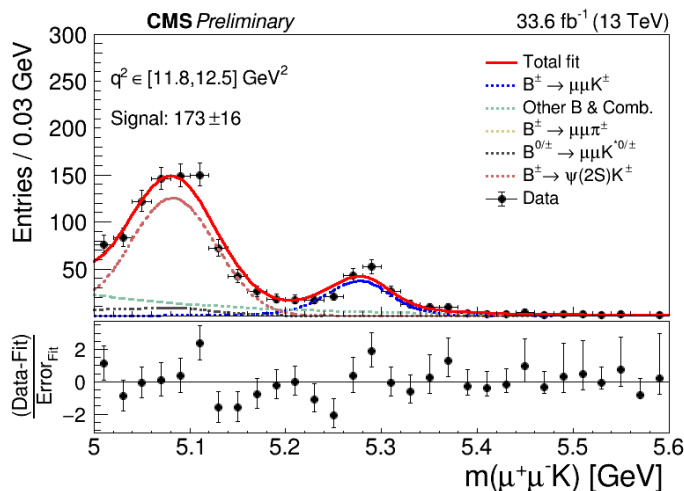
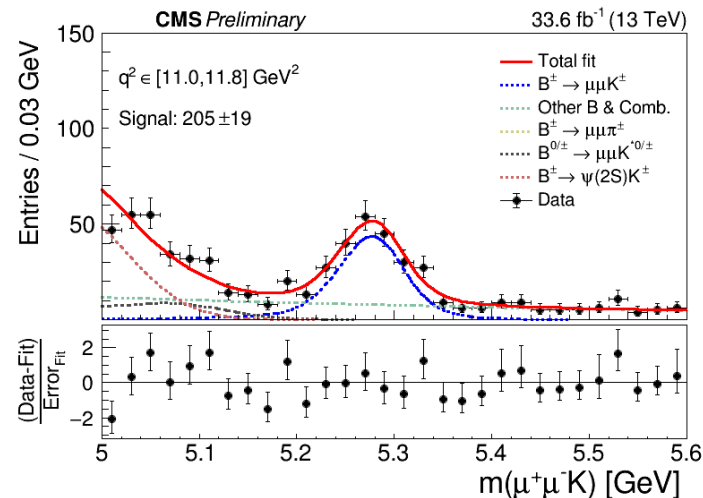
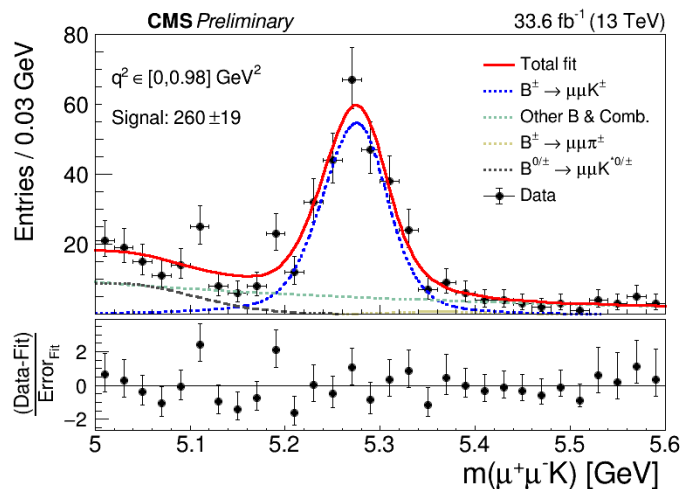
- Since adequate statistics available: differential measurement, dBF/dq^2
- Use the same selection and code and instead for a single fit, do a simultaneous fit in q^2 bins
- Result to be compared with several theoretical predictions

Bin	q^2 range [GeV ²]
1	0–0.98
2	1.1–2.0
3	2.0–3.0
4	3.0–4.0
5	4.0–5.0
6	5.0–6.0
7	6.0–7.0
8	7.0–8.0
9	11.0–11.8
10	11.8–12.5
11	14.82–16.0
12	16.0–17.0
13	17.0–18.0
14	18.0–19.24
15	19.24–22.9

B \rightarrow $\mu\mu$ K mass fits in q^2 bins

Rest of the fits in back up

Bin	q^2 range [GeV ²]
1	0–0.98
2	1.1–2.0
3	2.0–3.0
4	3.0–4.0
5	4.0–5.0
6	5.0–6.0
7	6.0–7.0
8	7.0–8.0
9	11.0–11.8
10	11.8–12.5
11	14.82–16.0
12	16.0–17.0
13	17.0–18.0
14	18.0–19.24
15	19.24–22.9



Main analysis

- Corrections on MC to account for known disagreements with data:
 - Trigger response, lepton reconstruction/identification, B p_T spectrum, BDT response
- Systematics are treated as independent between the muon and electron part of R_K
- The total uncertainty of R_K is dominated by the statistical part of electron channels

Uncertainties on the muon part

Source	Impact on the $R(K)$ ratio [%]
Background description, low- q^2 bin	1.75
Trigger turn-on	1.30
Reweighting in p_T and rapidity	0.86
Background description, J/ψ CR	0.64
J/ψ meson radiative tail description	0.48
Pileup	0.38
Signal shape description	0.32
Trigger efficiency	0.16
J/ψ resonance shape description	0.08
Nonresonant contribution to the J/ψ CR	0.07
Total systematic uncertainty	2.5
Statistical uncertainty in MC samples	1.7
Statistical uncertainty	7.5
Total uncertainty	8.1

Uncertainties on the electron part

Source	Impact on the $R(K)$ ratio [%]	
	PF-PF	PF-LP
Signal and background description	5	5
J/ψ event leakage to the low- q^2 bin	4	9
BDT efficiency stability	2	5
BDT cross validation	2	3
Trigger efficiency	1	4
BDT data/simulation difference	1	2
J/ψ meson radiative tail description	1	1
Total systematic uncertainty	7	13
Statistical and total uncertainty	40	200

Systematic uncertainties and corrections



- Corrections on MC to account for known disagreements with data:
 - Trigger response, lepton reconstruction/identification, B p_T spectrum, BDT response
- Systematics are treated as independent between the muon and electron part of R_K
- The total uncertainty of R_K is dominated by the statistical part of electron channels

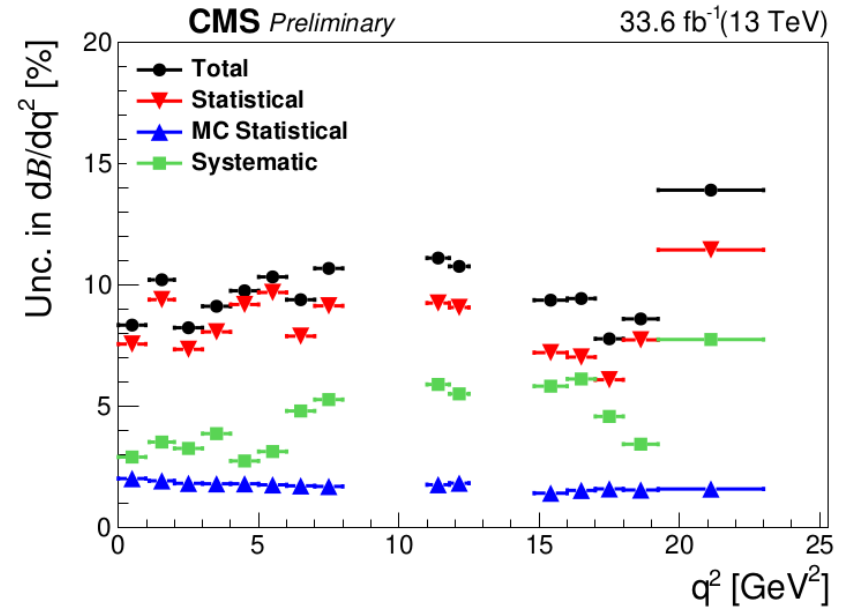
Uncertainties on the muon part

Uncertainties on the electron part

Source
Background
Trigger t
Reweight
Background
J/ ψ meso
Pileup
Signal sh
Trigger e
J/ ψ reson
Nonreson
Total syst
Statistica
Statistica
Total unc

- Same uncertainty sources considered for the single-bin muon measurement, are evaluated in each q^2 bin

- In all bins: total uncertainty is dominated by the statistical component



Results

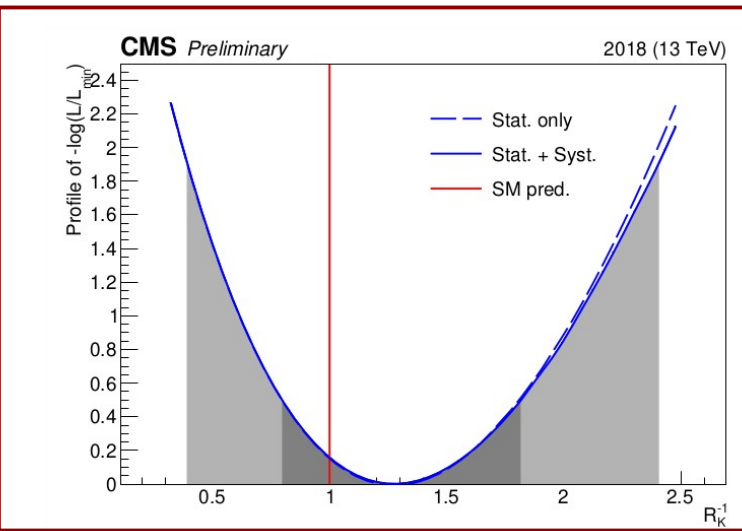
BF(B→μμK) and R_K in the low q²

BF(B→ μμK) in full low-q² range (1.1 < q² < 6.0 GeV²):

BF (B[±] → K[±]μ⁺μ⁻) , 1.1 < q² < 6.0 GeV²
= (1.242 ± 0.054 (stat) ± 0.011 (MC stat) ± 0.040 (syst)) × 10⁻⁷

Can be compared with the various theoretical predictions

Package	EOS	Flavio	HEP fit	SuperIso
Prediction [×10 ⁻⁷]	1.89 ±0.13	1.71 ±0.27	1.98 ±0.73	1.65 ±0.34



Central value and confidence range by minimizing the Likelihood fit function of R_K⁻¹:

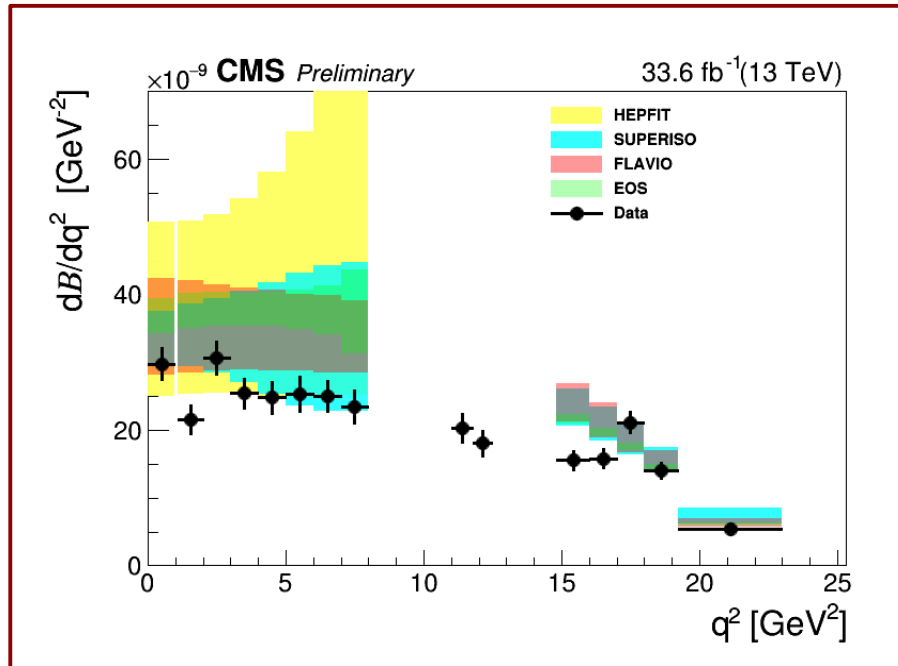
R_K = 0.78^{+0.46}_{-0.23} (stat) ^{+0.09}_{-0.05} (syst)

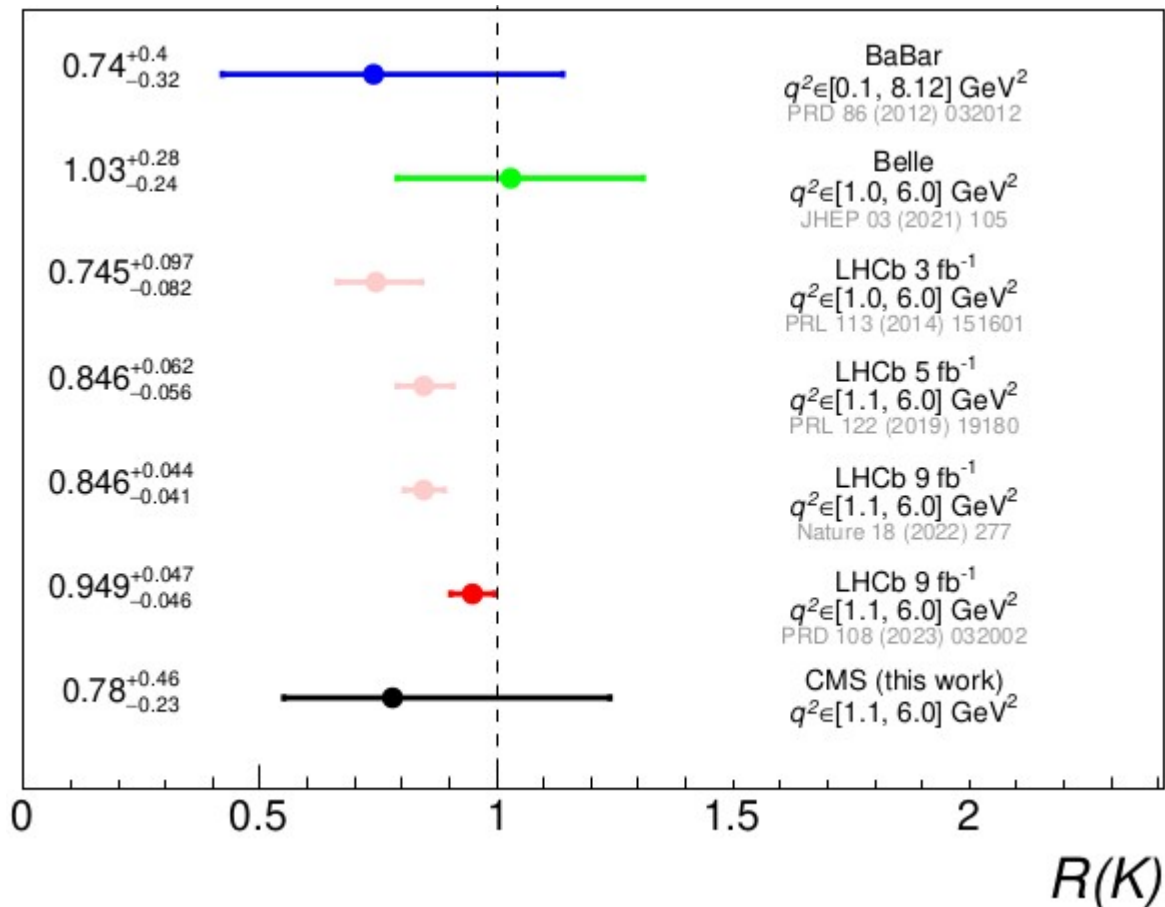
Precision dominated by the low stats of B → eeK

Measurement of differential BF($B \rightarrow \mu\mu K$)

- For differential BR measurement, a fit is performed in all q^2 bins at the same time
- Compare measurement with the theoretical predictions in each q^2 bin

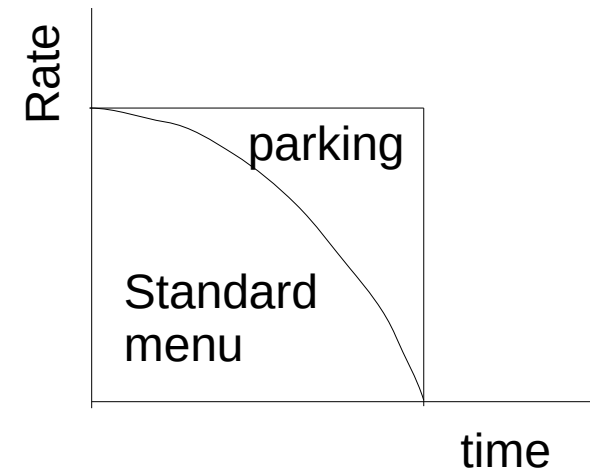
Measurement of dBR/dq^2 and comparison with theory





- Lessons learned from Run 2 (up to 2018):
 - Muon channel: high statistics → comparable precision to world average
 - Electron channel: low statistics → “penalty” for using the “probe B”

- In Run 3 (after 2022) we improved the strategy:
 - Two parking samples used (one for muons/ one for electrons)
 - Same strategy of exploiting the unused L1/HLT rate:
 - Gradually enabling looser triggers
 - Dielectron parking is based on:
 - Topological variables
 - p_T thresholds
 - Sophisticated online ID
 - Expecting large increase in stats
 - **Analysis is ongoing; first look quite promising...**



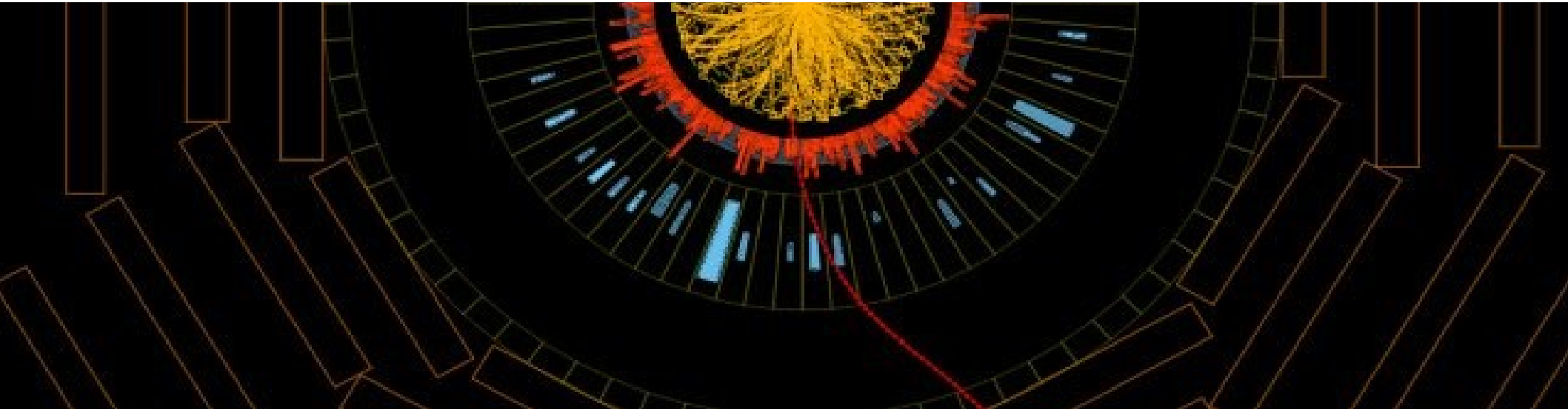
Summary



- CMS pursuing a very ambitious B Physics program
- First RK result using 2018 data demonstrates the robustness and adaptability of the CMS detector, trigger and software
 - We improved triggering strategy in Run 3
 - **Expecting large increase in statistics of $B \rightarrow eeK$**

Public analysis summary is posted here: [BPH 22-005](#)

Stay tuned for more!

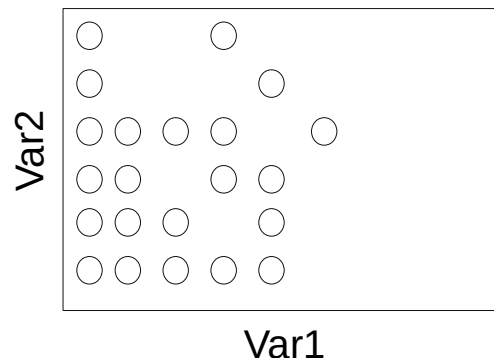


Back up

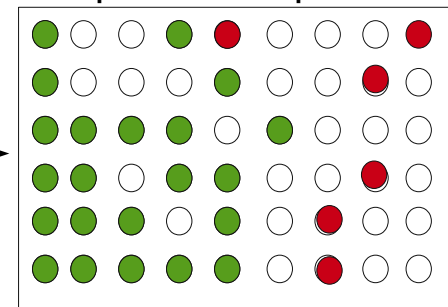
Adaptive grid search:

- Every variable is a dimension
- Scan variables (grid points)
- Take into account previous searches before generating a point
- Find optimal, according to some metric(s)
- Computing resources reduced by $\sim 75\%$ wrt to standard grid search

Step1: Generate points



Step2: use previous result to skip useless points



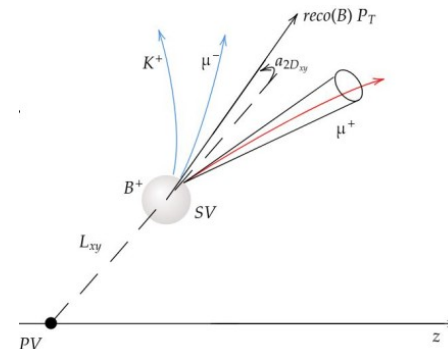
- Generated now
- Previous generation
- Excluded

Preselection for $\mu\mu K$:

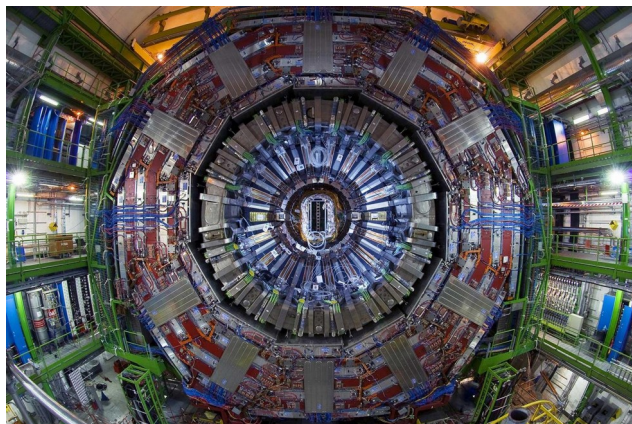
- $p_T(B) > 3 \text{ GeV}$
- $\Delta z(\text{trg } \mu, \text{ track}/\mu^2) < 1.0 \text{ cm}$
- $p_T(\text{track}) > 1 \text{ GeV}$
- $L_{xy}/\sigma > 1$
- $\cos(\alpha) > 0.90$
- $\text{Prob} > 10^{-5}$
- $m(K, \mu) > 2 \text{ GeV}$ [anti- D^0]

Preselection for eeK :

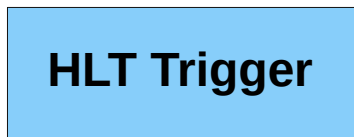
- $\Delta z(\text{trg } \mu, \text{ track}/e) < 1.0 \text{ cm}$
- $p_T(e2) > 1.0 \text{ GeV}$
- $\cos(\alpha) > 0.95$
- $\text{Prob} > 10^{-5}$
- $m(K, e) > 2 \text{ GeV}$ [anti- D^0]
- $d_{3d} < 0.06$
- $\text{ID}(e1) > -2$
- $\text{ID}(e2) > 0$



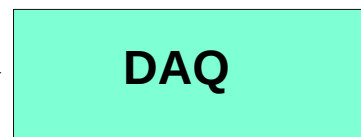
Collisions (p - p) at 40 MHz



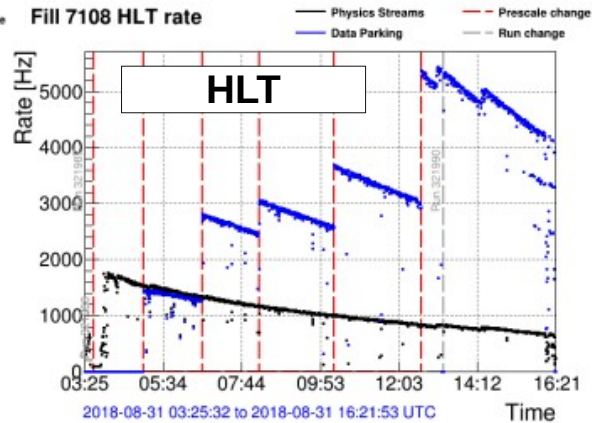
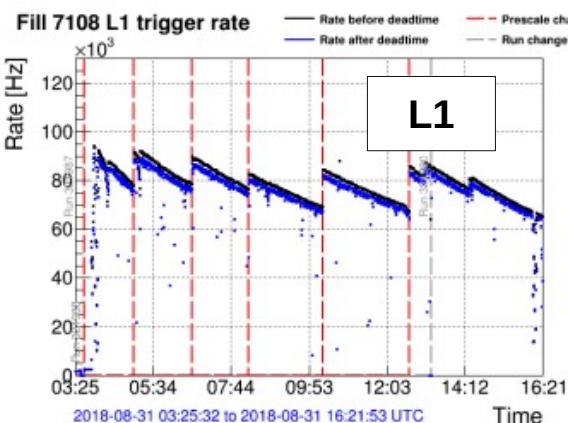
- Single- μ L1 seeds
- η restricted, soft p_T
- Purity in B decays $\sim 30\%$
- Constant L1 rate



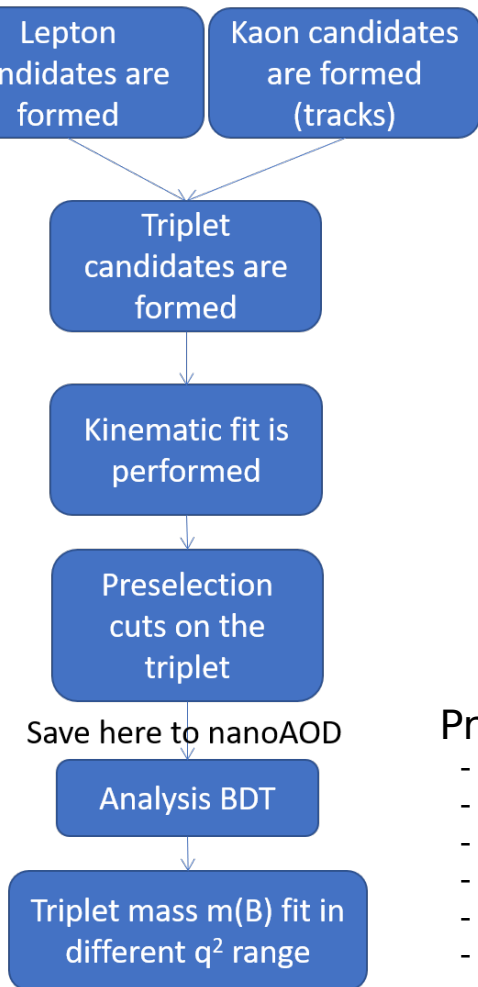
- L1 seeds as inputs
- Refined p_T and d_{xy} cut



- Saved in single copy
- Stored on tape until computing resources available
- Long delay in reconstruction; procedure known as "Parking"



- As luminosity decreases lower p_T seeds enabled
- Tune/optimize paths during data-taking
- **Collected during 2018**



A practical problem: Running on 10^{10} events needs a lot of storage, time and computing power

Code strategies:

- 1) Apply cuts as quickly as possible in every step of the reconstruction
- 2) Move time consuming processes to the end of the chain

Algorithm:

- Select leptons of opposite sign and create the common vertex
- Combine with a track (Kaon mass assigned)
- Kinematic Fit to a common vertex

Preselection:

- Adaptive grid search approach used
- Cut values are different for $\mu\mu K$ and eeK

Preselection for $\mu\mu K$:

- $p_T(B) > 3 \text{ GeV}$
- $\Delta z(\text{trg } \mu, \text{ track}/\mu^2) < 1.0 \text{ cm}$
- $p_T(\text{track}) > 1 \text{ GeV}$
- $L_{xy}/\sigma > 1$
- $\cos(\alpha) > 0.90$
- $\text{Prob} > 10^{-5}$
- $m(K, \mu) > 2 \text{ GeV}$ [anti- D^0]

Preselection for eeK :

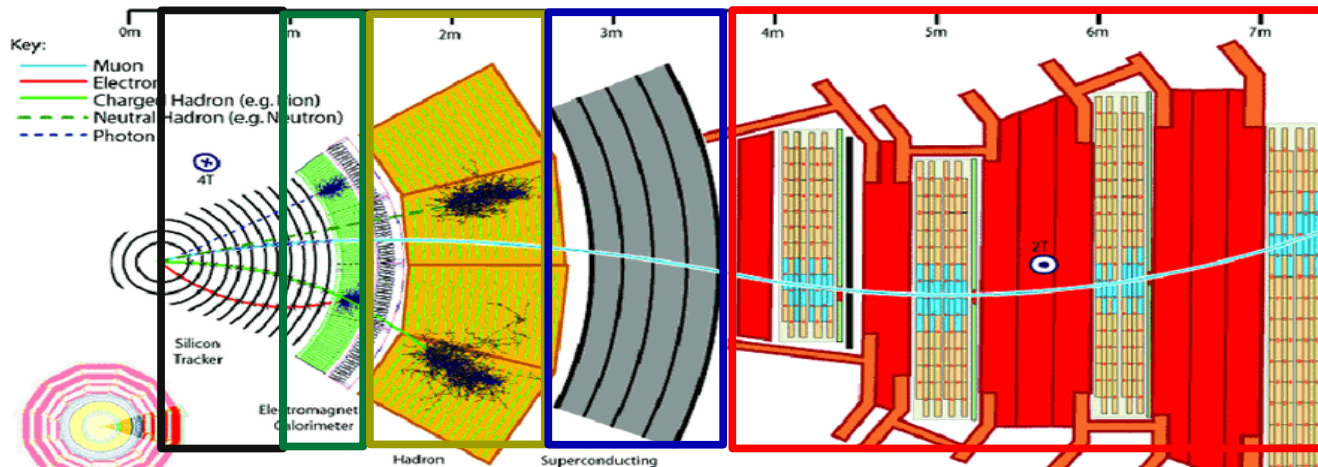
- $\Delta z(\text{trg } \mu, \text{ track}/e) < 1.0 \text{ cm}$
- $p_T(e2) > 1.0 \text{ GeV}$
- $\cos(\alpha) > 0.95$
- $\text{Prob} > 10^{-5}$
- $m(K, e) > 2 \text{ GeV}$ [anti- D^0]
- $d_{3d} < 0.06$
- $\text{ID}(e1) > -2$
- $\text{ID}(e2) > 0$

Yields

Bin	q^2 range [GeV]	Branching fraction [10^{-8}]
1	0–0.98	2.98 ± 0.25
2	1.1–2.0	2.15 ± 0.22
3	2.0–3.0	3.07 ± 0.25
4	3.0–4.0	2.54 ± 0.23
5	4.0–5.0	2.48 ± 0.24
6	5.0–6.0	2.53 ± 0.26
7	6.0–7.0	2.51 ± 0.23
8	7.0–8.0	2.35 ± 0.25
9	11.0–11.8	2.03 ± 0.22
10	11.8–12.5	1.80 ± 0.19
11	14.82–16.0	1.55 ± 0.14
12	16.0–17.0	1.58 ± 0.15
13	17.0–18.0	2.11 ± 0.16
14	18.0–19.24	1.40 ± 0.12
15	19.24–22.9	0.53 ± 0.07

The Compact Muon Solenoid detector

More information in the [TDR](#)



- Tracker:**
- Pixels in the core
 - Silicon strips around
 - In 2017 an extra inner layer added
 - Total 14(15) layers in Barrel(endcaps)
 - Reconstructs the trajectory of charged particles
 - Excellent measurement of position

- ECAL:**
- Homogeneous calorimeter
 - Lead tungstate (PbWO) scintillator
 - 61,200 crystals in barrel
 - 1,700 crystals in endcap
 - Measures the energy of e and γ
 - Very good energy resolution

- HCAL:**
- Heterogeneous calorimeter
 - Interleaved heavy material with scintillator layers
 - Measures the energy of hadrons
 - Indirect measurement of non-interacting particles (like ν)

- Magnet:**
- Central device
 - Large solenoid magnet
 - Field up to 4T
 - Bends charged particles to measure their momentum

- Muon:**
- Position exploits the penetration of muons
 - Very clean signatures
 - Gaseous detectors of three types
 - Drift tubes (barrel), CSC (endcap), RPC (barrel+endcap)

BDT leplepK common variables

$\cos \alpha_{3D}$	Cosine of the angle between the momentum vector of the B^+ candidate and the vector connecting the PV and SV
$p(B^+ \text{ vtx})$	Probability of the SV kinematic fit
L_{xy}/σ_{xy}	Significance of the SV displacement in the transverse plane with respect to the PV
$p_T(B^+)$	Transverse momentum of the B^+ candidate; in the electron channel it is divided by $m_{K^+e^+e^-}$
$p_T(K^+)$	Transverse momentum of the K^+ candidate; in the electron channel it is divided by $m_{K^+e^+e^-}$

BDT $\mu\mu K$ exclusive variables

$\min \Delta R(\mu, K^+)$	$\Delta R = \sqrt{(\Delta\eta)^2 + (\Delta\phi)^2}$ distance between the K^+ candidate and the closest muon
$\min \Delta z(\mu, K^+)$	Δz distance between the points of origin of the K^+ candidate and the closest muon along the beam axis direction
$\text{Iso}(\mu_{\text{lead}})$	PF isolation for the p_T -leading muon, defined as a scalar p_T sum all PF candidates, excluding the muon itself, within $\Delta R < 0.4$ of the muon and corrected for PU

BDT eeK exclusive variables

$$p_T(e_{1,2})m_{K^+e^+e^-}$$

Transverse momenta of the two electron candidates, divided by the invariant mass of the B^+ candidate

$$\Delta z(e_{1,2}, K^+)$$

Longitudinal distance between the points of origin of each electron and the kaon

$$|d_{3D}(K^+, e^+e^-)|/\sigma_{|d_{3D}(K^+, e^+e^-)|}$$

Kaon 3D impact parameter significance with respect to the dielectron vertex

$$\Delta R(e^+, e^-)$$

ΔR between the two electrons

$$\Delta R(e_{1,2}, K^+)$$

ΔR between each electron and the kaon

$$\frac{|\mathbf{p}(e^+e^-) \times \mathbf{r}| - |\mathbf{p}(K^+) \times \mathbf{r}|}{|\mathbf{p}(e^+e^-) \times \mathbf{r}| + |\mathbf{p}(K^+) \times \mathbf{r}|}$$

Asymmetry of the momentum of the dielectron system and that of the K^+ momentum with respect to the B^+ candidate trajectory, where \mathbf{r} is a unit vector connecting the PV and SV

$$ID(e_{1,2})$$

Electron ID BDT score for each of the two electrons

$$I_{\Delta R=0.4}^{\text{rel}}(e_1/e_2/K^+)$$

Relative track-based isolation of e_1 , e_2 , and K^+ candidates, respectively, defined as a scalar p_T sum of all additional tracks in a $\Delta R < 0.4$ cone around the candidate, divided by the candidate's p_T

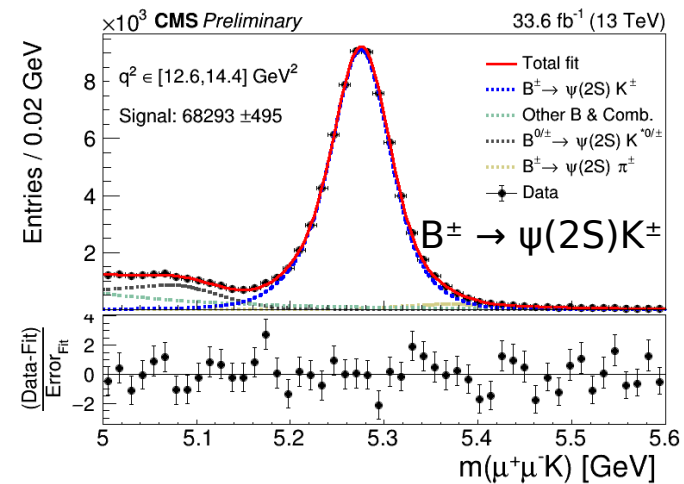
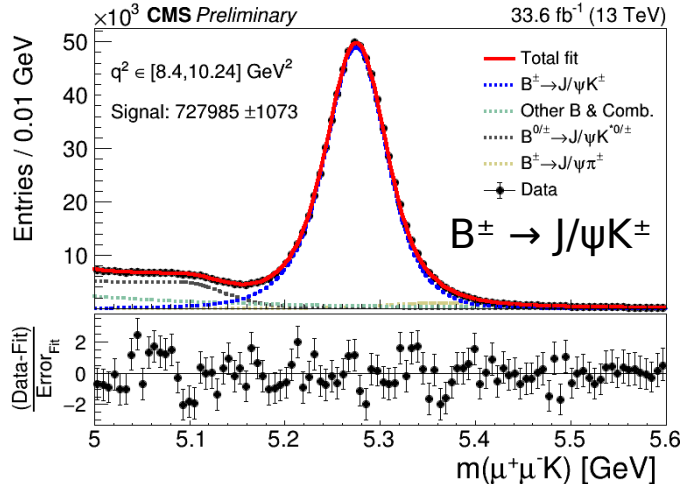
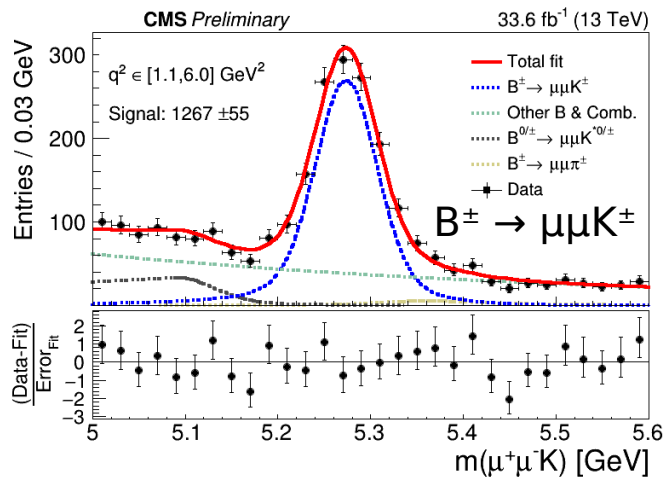
B → μμX mass fits

Functions used for each fit component per decay

	$B^\pm \rightarrow \mu\mu K^\pm$	$B^\pm \rightarrow J/\psi K^\pm$	$B^\pm \rightarrow \psi(2S)K^\pm$
Signal	DSCB + Gaussian	Sum of 3 Gaussians	DSCB + Gaussian
Comb & other B	Exponential	Exponential	Exponential
$B^\pm \rightarrow K^{*0/\pm} X$	DSCB	DSCB + Exponential	DSCB + Exponential
$B^\pm \rightarrow \pi^\pm X$	DSCB	DSCB	DSCB

Where $X=J/\psi, \psi(2S), \mu\mu$

DSCB = Double-Sided Crystal Ball



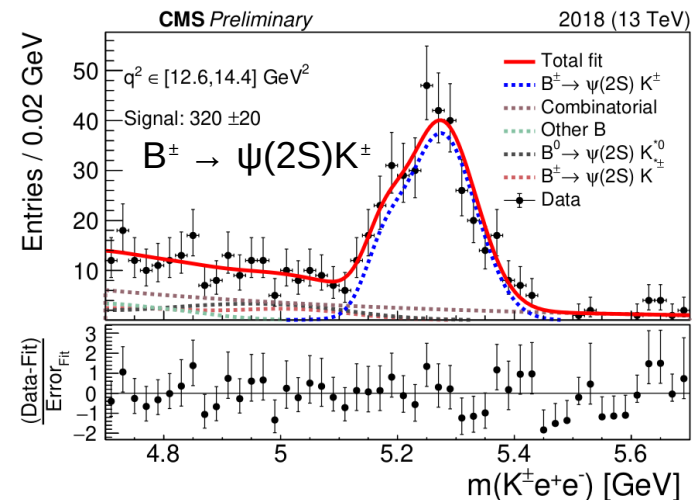
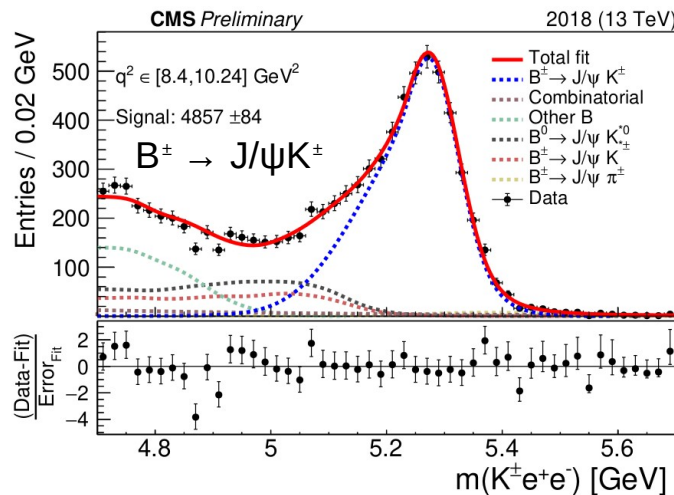
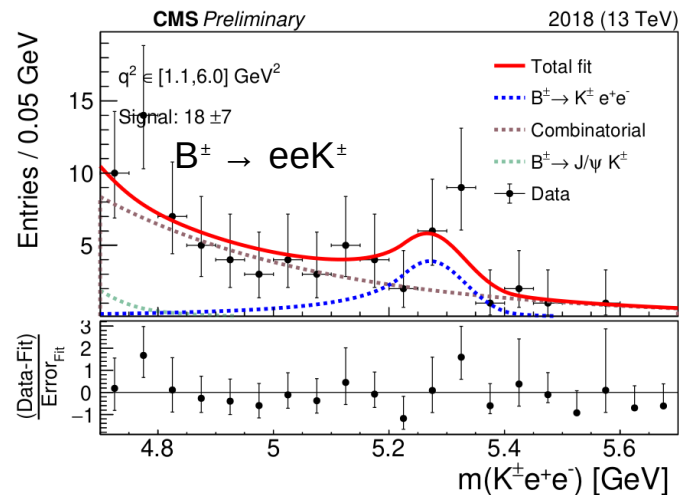
B → eeX mass fits (PF - PF)

Functions used for each fit component for 2 PF electron channels

	$B^{\pm} \rightarrow eeK^{\pm}$	$B^{\pm} \rightarrow J/\psi K^{\pm}$	$B^{\pm} \rightarrow \psi(2S)K^{\pm}$
Signal	DSCB	CB + Gaussian	CB + Gaussian
Combinatorial/Other B	Exponential / -	Exponential / KDE	Exponential / KDE
$B^{\pm} \rightarrow K^{*0/\pm} X$	-	KDE template	KDE template
$B^{\pm} \rightarrow \pi^{\pm} X$	-	CB	-
$B^{\pm} \rightarrow J/\psi K^{\pm}$	KDE template	-	-

Where X=J/ψ, ψ(2S), ee

KDE = Kernel Density Estimator, CB = Crystal Ball, DSCB = Double-Sided Crystal Ball



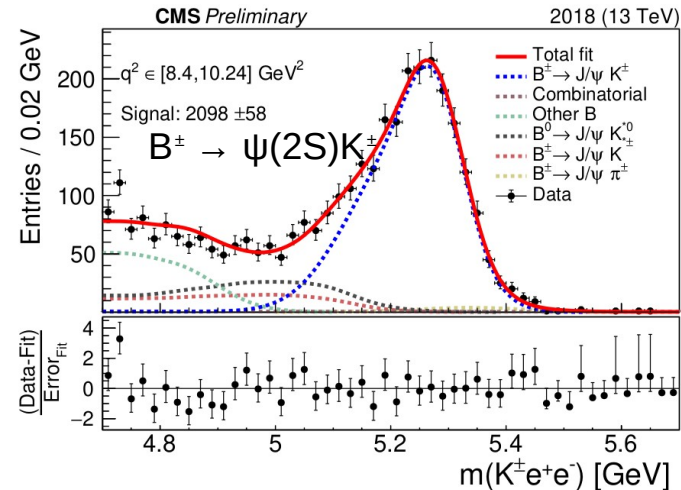
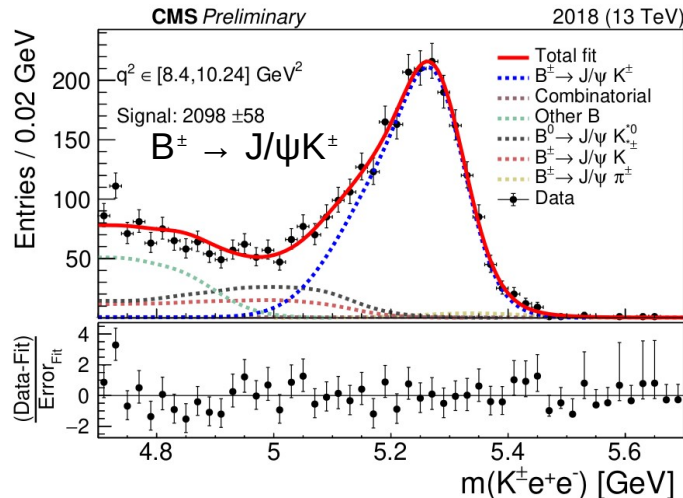
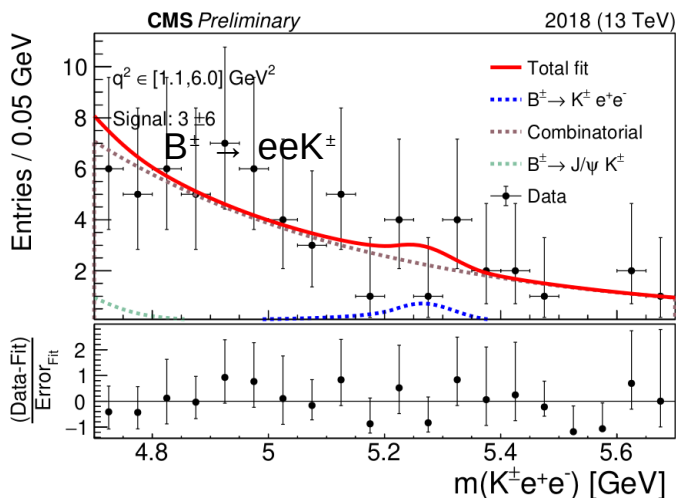
B → eeX mass fits (PF - LP)

Functions used for each fit component for PF - LP electron channels

	$B^\pm \rightarrow eeK^\pm$	$B^\pm \rightarrow J/\psi K^\pm$	$B^\pm \rightarrow \psi(2S)K^\pm$
Signal	DSCB	CB + Gaussian	CB + Gaussian
Combinatorial/Other B	Exponential / -	Exponential / KDE	Exponential / KDE
$B^\pm \rightarrow K^{*0/\pm} X$	-	KDE template	KDE template
$B^\pm \rightarrow \pi^\pm X$	-	CB	-
$B^\pm \rightarrow J/\psi K^\pm$	KDE template	-	-

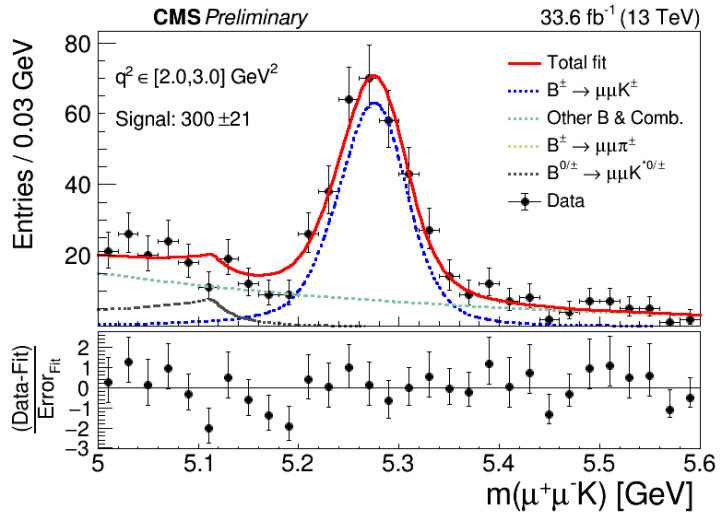
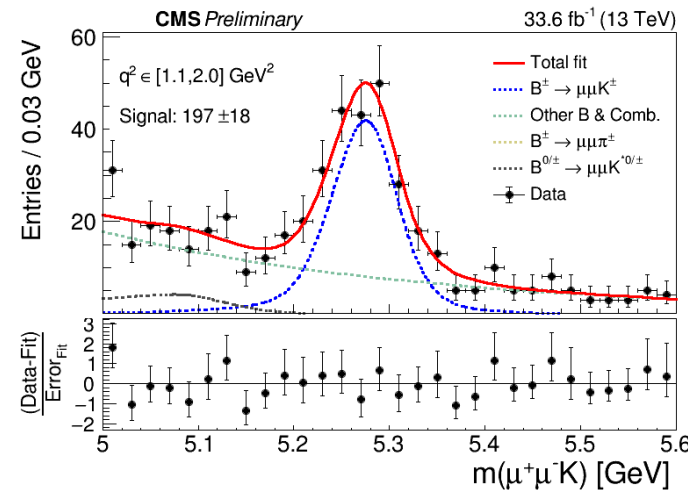
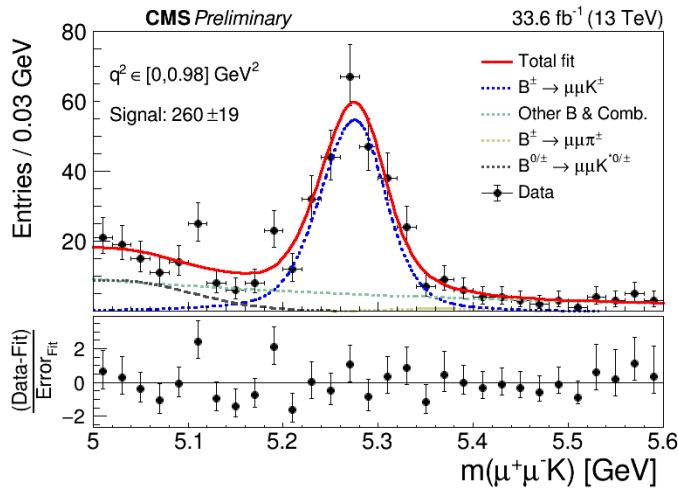
Where X=J/ψ, ψ(2S), ee

KDE = Kernel Density Estimator, CB = Crystal Ball, DSCB = Double-Sided Crystal Ball



B → μμK mass fits in q² bins

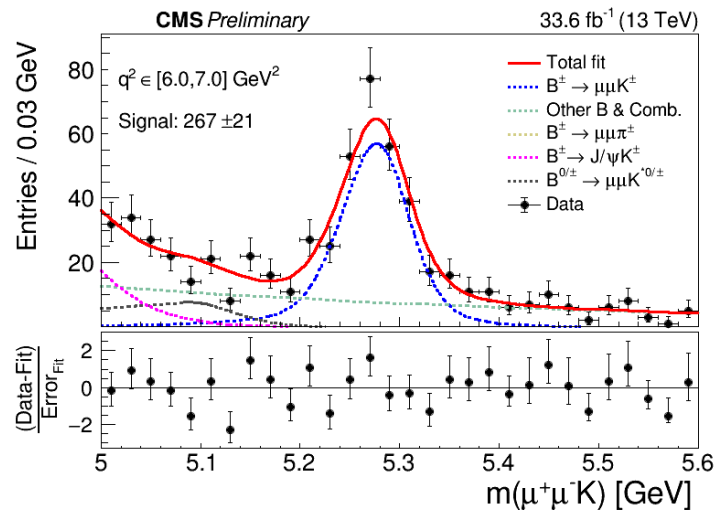
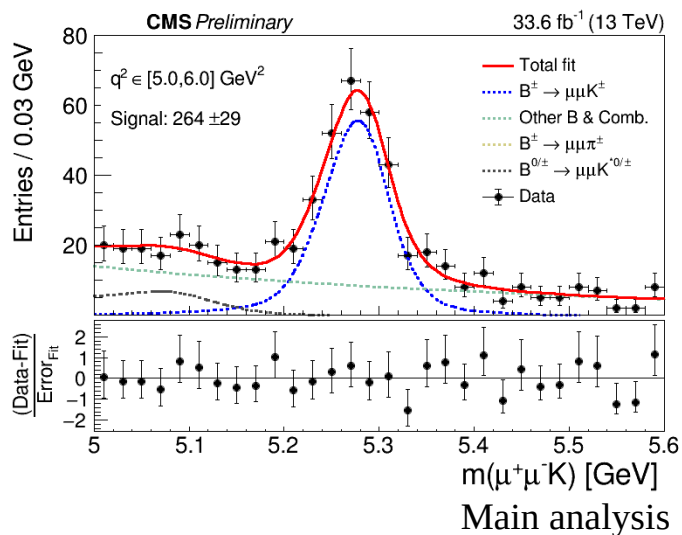
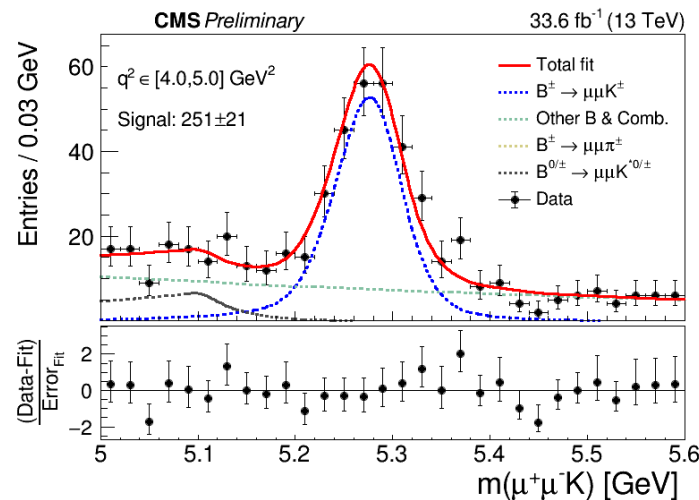
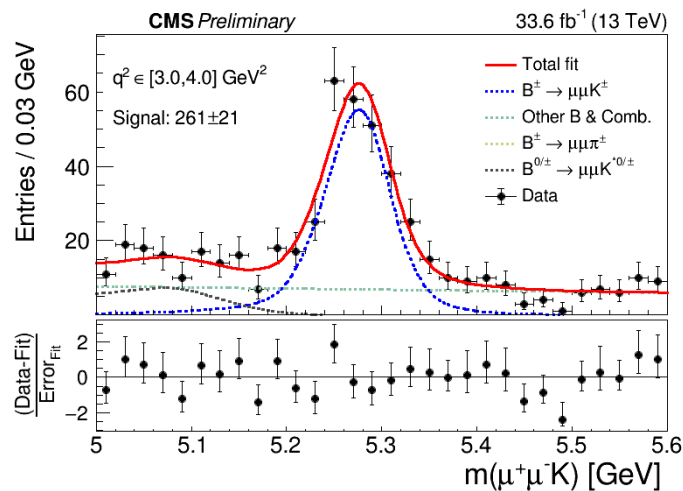
Bin	q ² range [GeV ²]
1	0–0.98
2	1.1–2.0
3	2.0–3.0
4	3.0–4.0
5	4.0–5.0
6	5.0–6.0
7	6.0–7.0
8	7.0–8.0
9	11.0–11.8
10	11.8–12.5
11	14.82–16.0
12	16.0–17.0
13	17.0–18.0
14	18.0–19.24
15	19.24–22.9



Main analysis

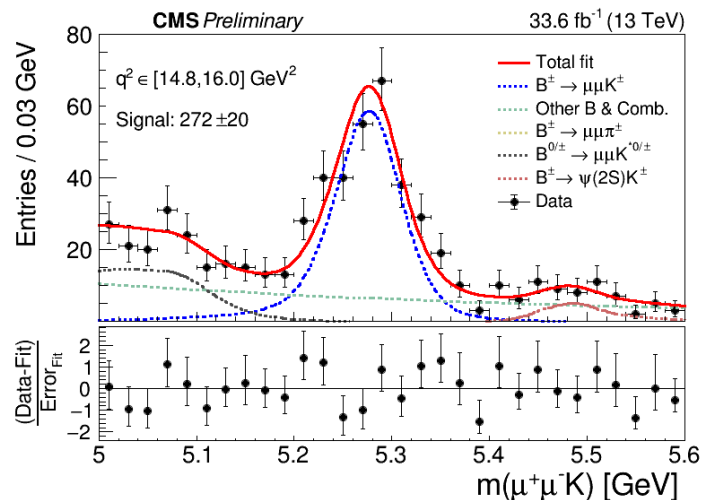
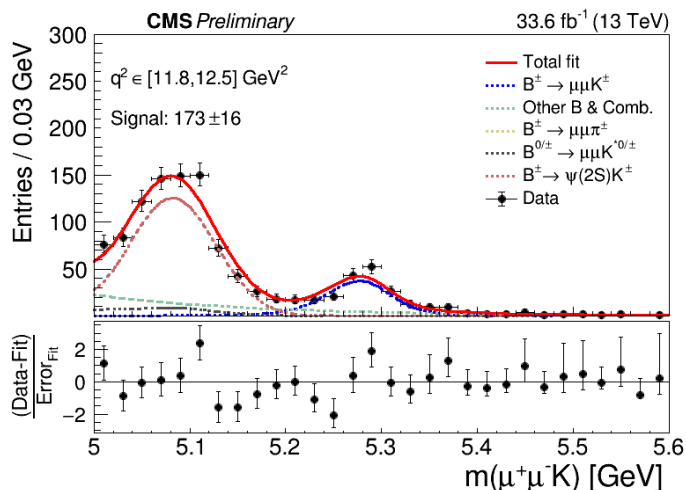
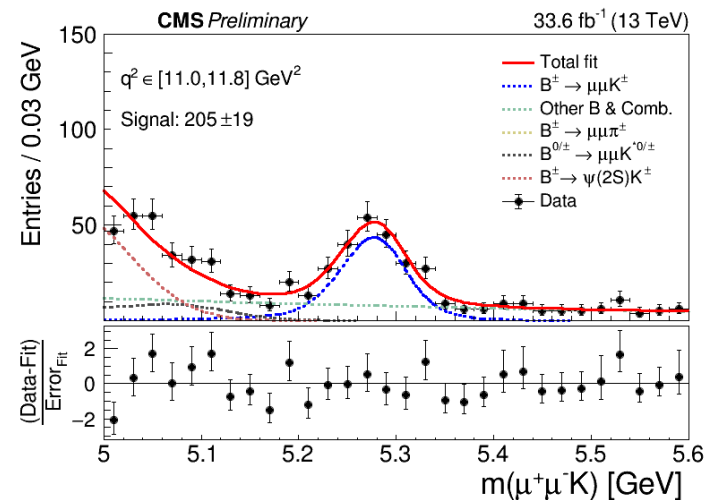
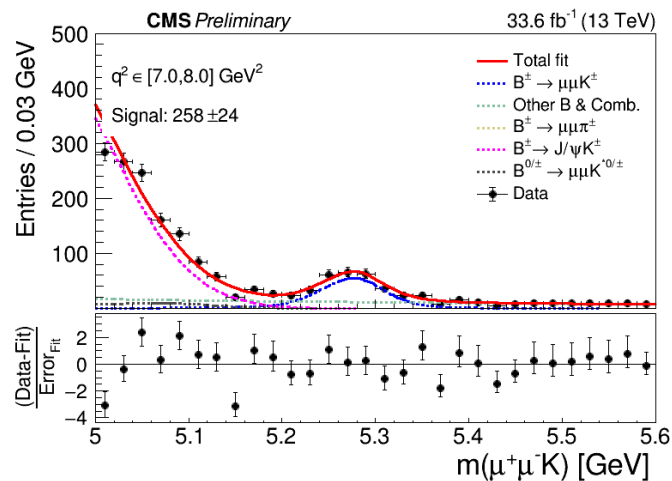
B \rightarrow $\mu\mu$ K mass fits in q^2 bins

Bin	q^2 range [GeV 2]
1	0–0.98
2	1.1–2.0
3	2.0–3.0
4	3.0–4.0
5	4.0–5.0
6	5.0–6.0
7	6.0–7.0
8	7.0–8.0
9	11.0–11.8
10	11.8–12.5
11	14.82–16.0
12	16.0–17.0
13	17.0–18.0
14	18.0–19.24
15	19.24–22.9



B → μμK mass fits in q² bins

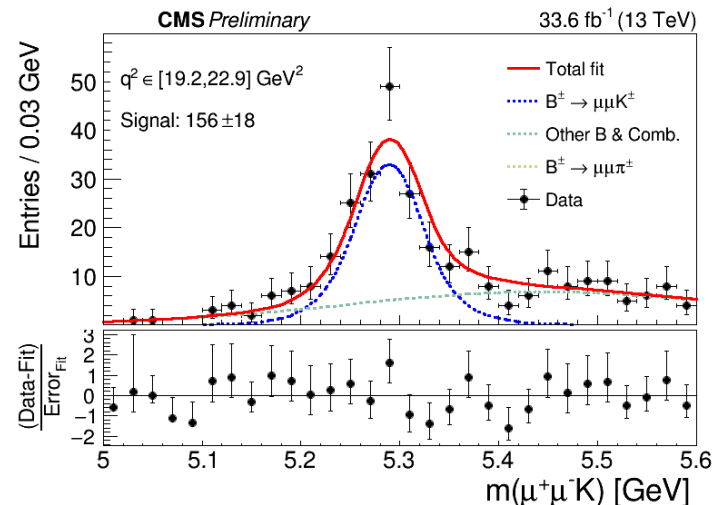
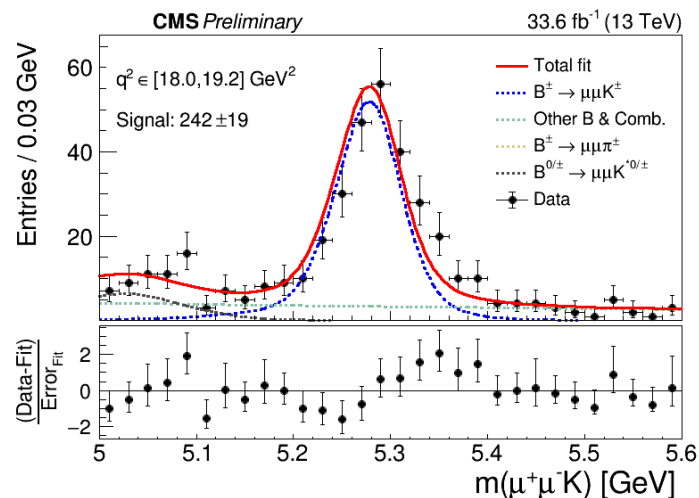
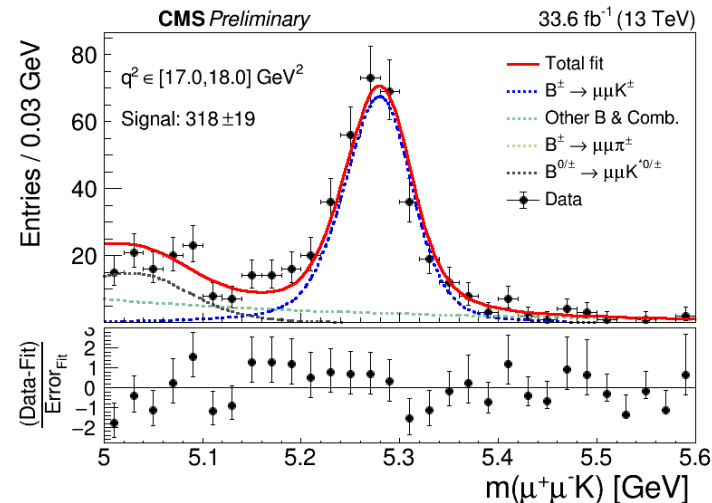
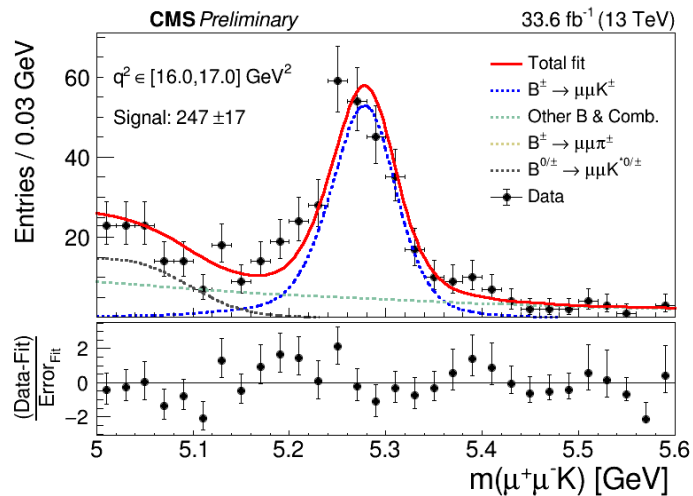
Bin	q ² range [GeV ²]
1	0–0.98
2	1.1–2.0
3	2.0–3.0
4	3.0–4.0
5	4.0–5.0
6	5.0–6.0
7	6.0–7.0
8	7.0–8.0
9	11.0–11.8
10	11.8–12.5
11	14.82–16.0
12	16.0–17.0
13	17.0–18.0
14	18.0–19.24
15	19.24–22.9



Main analysis

B → μμK mass fits in q² bins

Bin	q ² range [GeV ²]
1	0–0.98
2	1.1–2.0
3	2.0–3.0
4	3.0–4.0
5	4.0–5.0
6	5.0–6.0
7	6.0–7.0
8	7.0–8.0
9	11.0–11.8
10	11.8–12.5
11	14.82–16.0
12	16.0–17.0
13	17.0–18.0
14	18.0–19.24
15	19.24–22.9



Main analysis